DEVELOPMENT OF NANOMATERIALS IN COMBINATION WITH BIO-SORBENT FOR POTENTIAL APPLICATION IN WATER REMEDIATION

A DISSERTATION

Submitted in partial fulfilment of the requirements
for the award of the degree of

MASTER OF TECHNOLOGY

in

BIOPROCESS ENGINEERING

by

MADHULIKA NARAYAN

DEPARTMENT OF BIOTECHNOLOGY

INDIAN INSTITUTE OF TECHNOLOGY ROORKEE
ROORKEE – 247 667 (INDIA)

MAY, 2019

DEVELOPMENT OF NANOMATERIALS IN COMBINATION WITH BIO-SORBENT FOR POTENTIAL APPLICATION IN WATER REMEDIATION

A DISSERTATION

Submitted in partial fulfilment of the requirements
for the award of the degree of

MASTER OF TECHNOLOGY

in

BIOPROCESS ENGINEERING

by

DEPARTMENT OF BIOTECHNOLOGY
INDIAN INSTITUTE OF TECHNOLOGY ROORKEE
ROORKEE-247 667 (INDIA) MAY, 2019

CANDIDATE'S DECLARATION

I hereby declare that the work presented in dissertation entitled **"DEVELOPMENT OF NANOMATERIALS IN COMBINATION WITH BIO-SORBENT FOR POTENTIAL APPLICATION IN WATER REMEDIATION"** submitted in partial fulfillment of the requirements for the award of degree of **Master of Technology** in **Bioprocess engineering**, **Indian Institute of Technology Roorkee**, is an authentic record of my work carried out under the supervision of **Dr. P. Gopinath**, Associate Professor, Department of Biotechnology, IIT Roorkee.

The matter embodied in this work has not been submitted by me for the award of any other degree.

Madhulika Narayan
Enrolment No. 17559002
Date:

CERTIFICATE

This is to certify that the above statement made by the candidate is correct to the best of my knowledge.

Dr. P. Gopinath
Supervisor
Associate Professor
Department of Biotechnology
Indian Institute of Technology Roorkee

ABSTRACT

The integration of polymers with biomaterials offers promising and effective nanomaterials with intrinsic and extrinsic properties that are utilized in several applications namely tissue engineering, drug delivery, energy storage, sensors, environmental remediation etc. The present thesis reported the development of such polymer supported bio-sorbent (*Moringa oleifera,* (MO)) which was utilized for the application in water remediation. Owing to the industrialization, the water bodies are severely contaminated due to the uncontrolled discharge of industrial effluents i.e. specifically the dye pollutants from textile and tanning industries which are highly toxic and carcinogenic. This dissertation work was carried out by taking the pragmatic approach by the unique fabrication methodologies and developed two different forms of adsorbents i.e. the first one is the MO encapsulated sodium alginate (Na Alg/MO) beads and the latter represents the MO loaded polyacrylonitrile (PAN/MO) nanofibers. The former Na Alg/MO beads was synthesized by cross linking method and the latter was prepared by solvent homogenization method followed by the deposition of nanofibers through electrospinning method. The developed bio-sorbents were characterized by several analytical and spectroscopic techniques in order to investigate the material properties along with their control counterparts. The techniques used for the investigation are FESEM, TEM, XRD, FTIR, XPS. Further the batch adsorption experiments were performed for each adsorbent. The studies include effect of contact time, percentage removal, adsorption capacity, effect of pH and finally the reusability studies. The adsorption data are validated using the empirical equations of the pseudo-kinetic first order and pseudo-second order models. Similarly, the mechanism involved in the adsorption phenomena was investigated by the isothermal studies namely Langmuir and Freundlich models, respectively. The obtained model results and its parameters were compared with the experimental data and discussed. It was ascertained from the results that both the forms of adsorbents are effective in adsorption of Congo red (CR) dye. But considering the practical implications, it was suggested to utilize the bio-sorbents in the nanofibers form which will be beneficial for the commercialization in future. In a nutshell, this work corroborated the importance of bio-based natural materials available in nature and how it can be effectively engineered with the recent polymeric materials for obtaining novel hybrid materials with excellent properties for various applications.

LIST OF FIGURES

LIST OF FIGURES

ABBREVIATIONS

%.....	Percentage
cm…….	Centimetre
CNTs……	Carbon Nanotubes
C_e…….....	Equilibrium concentration
CR……	Congo Red
FESEM…….	Field emission Scanning electron microscope
FTIR…….	Fourier transform infrared spectroscopy
K_L.....	Langmuir constant
K_f.....	Freundlich constant
Mg……	milligram
MO…….....	Moringa oleifera
NaAlg/MO……...	Sodium Alginate/Moringa oleifera
PAN…….	Polyacrylonitrile
PAN/MO……..	Silver nanoparticles
pH…….	Potential of hydrogen
Ppm……..	Parts per million
R_L……	Separation factor
TEM…….	Transmission electron microscope
Q_e…….....	Equilibrium adsorption capacity
Q_m……...	D-R monolayer adsorption capacity
Q_{max}……...	Maximum adsorption capacity
Q_t…….....	Adsorption capacity at a particular time t
XRD…….	X-ray Diffraction
XPS…….....	X-ray photoelectron spectroscopy
UV……	Ultraviolet

ACKNOWLEDGEMENTS

I would like to extend my sincere and heartfelt thanks to all my respected teachers, my colleagues as well as to my family and friends. Each of them has had an important role to play in the whole journey of my M. Tech thesis

First and foremost, I would like to thank Prof Gopinath Sir for his invaluable guidance, and constant, unwavering support. It was his encouragement that helped me to constantly experiment and learn during the entire M. Tech course. He was a true inspiration for me to give my best and to make the whole experience such an enriching and educative process.

I would like to thank all the professors of the Department of Bioprocess Engineering for their excellent teaching, advice and guidance, all of which will stay with me throughout my life. I would also like to thank the staff of IIC () and the entire staff for their ever efficient and timely help during the course of my project.

I would like to express my thanks to the Head of Department, Center for Nanotechnology, Prof R.K.Dutta and the Head of Department, Department of Biotechnology, Prof. A.K.Sharma for providing me ready access to all the laboratory facilities during the project.

I extend my sincere thanks to all the staff of the Center for Nanotechnology, especially, Mr. Rawan Pal, Mr.Vinod and Mr. Naresh for their constant and timely hands-on help during the laboratory course work.

I would like to express my sincere gratitude to Raj Kumar Sir for his constant, invaluable support. He was always approachable and would always be ready to clear any of our doubts, small or big. His proactive guidance throughout the project was greatly valuable. I would also like to thank my senior, Sandeep Sir for his kind and prompt guidance whenever I would go to him. Let me also profusely thank my lab partner, Vikash. He was always constructive with his helpful suggestions and prompt and responsive when needed. His sense of humor helped keep us in good spirits and made the whole experience that much more enjoyable. I would like to thank all my other lab mates as well as my classmates from Bioprocess Engineering for their support.

My parents and sister were a constant source of encouragement and support. Even though they were in Bangalore, their keen interest, involvement and concern in my thesis project boosted and inspired me to keep moving forward at all times. I would also like to thank my grandparents for their tremendous support and wisdom which has always guided me in my life.

Finally, it will be remiss on my part if I do not thank my friends Ipshita, Roopal, Indu and Sharvari for taking an active interest in my project life and for standing with me through thick and thin always.

The M. Tech thesis journey will always remain an invaluable part of my life for which I am truly thankful.

CHAPTER 1 INTRODUCTION

1.1 Introduction

Water is one of the most vital components of the ecosystem for the survival of living systems. It is therefore crucial to examine water systems so that we can improve the quality of water as it can affect the living systems either directly or indirectly. Nowadays, due to the increase in consumption of water and drastically increasing pollution, it is now crucial to manage the water quality by maintaining safe levels for the water to be used in specific applications. For example, in many parts of the world the concentration of arsenic is greater than the maximum permissible limit. The maximum contaminant level (MCL) for arsenic in drinking water as recommended by the World Health Organization (WHO) in India is 10 μg/L and is often exceeded (GonzálezHorta et al., 2015). There are various causes of water pollution such as disposal of dyes, heavy metals and organic pollutants. Because dyes have chemical structures that are rather complex, dyes are difficult to treat with waste treatment operations that are conventionally used. Even when dyes are released in smaller quantities, they can be highly undesirable. Additionally, the colour released by dyes into water makes it aesthetically unpleasant (Bharathi and Ramesh, 2013). They can have long lasting and perilous effects on exposed organisms, which depend on how concentrated dye is and the time of exposure. (Lade et al., 2015) The major problem of dyes is that they absorb as well as reflect sunlight that reaches the water and hamper photosynthesis of aquatic plants and in turn affect the aquatic ecosystem

These dyes are highly toxic and do not easily get mineralized under natural environmental conditions as most of the dyes are azo dyes contain the chromophoric azo group (-N=N-). On top of that, many dyes are considered to be carcinogenic and mutagenic. The dye industry was not very significant a few centuries ago. It was only with growing health concern, that people paid attention to the dye wastes. An indication to the magnitude of this problem can be understood from the fact that approximately two percent of dyes are released directly into aqueous streams. (Bharathi and Ramesh, 2013). With the increased stringent laws on industrial discharge and the adverse effects it has on health, it becomes our prerogative to treat this wastewater. Because they have many negative impacts and are widely distributed in the ecosystem, their separation and removal has become one of the important studies of water remediation. Thus, the need of the hour is the clear illustration of the risks of the dyes and

how the ecological components may be less exposed to them. If all these elements are seriously considered, then the technical use of colorants and the handling involved might be possible without much health danger.

Removal of dyes and heavy metal can be chemical, physical, and biological means. Physical ways incorporates sorption, natural action, and filtration/coagulation ways etc. Chemical ways comprise of ozonization, Fenton chemical agent, picture chemical change reactions whereas biological ways embody aerobic degradation, anaerobic degradation etc. However, they are all associated with disadvantages. The disadvantages of processes like filtration and coagulation is the sludge generation and the chemicals that need to be added to monitor the adsorption process is finding a suitable adsorbent which can be regenerated, of using the Fenton process is the that it produces sludge and a by-product as well which is usually iron hydroxide, of ozonation processes are that they are cost and energy intensive and furthermore have a tendency to form bromates. Nevertheless, among all the methods, adsorption was found to be effective, easy as well as cheap. Moreover, adsorption is preferred over other processes due to possible regeneration on selection of effective adsorbent, sludge free operation and recovery of the sorbet. Experimental studies have proven to us that they can be effective water remediation can happen using non-conventional adsorbents.

Another upcoming method of water remediation is use of nanomaterials. Nanomaterials are materials with dimensions of less than 100 nm. They possess innumerable unique properties such as high surface to volume ratio and efficient catalytic activities. They help purify water through various mechanisms such as adsorption, reducing the toxicity of a compound by transforming them and removing pathogens. Nanomaterials are being produced in various shapes and are incorporated into various composites as well as catalytic membranes. Some of the popular nanomaterials that we use for water remediation are carbon nanotubes, dendrimers, silver nanomaterials and nanofibers. The importance of nanofibers in adsorption are that it has they possess unique properties such as high specific surface area, high porosity such that pores are very fine. From research it has been found that nanomaterials and activated carbon possess comparable surface areas and adsorption capacities. However, nanomaterials surpass activated carbon in the economical aspect as they are required in lower amounts and can be synthesised at lower costs (Ghasemzadeh et al., 2014)

Further they possess properties such as extremely high surface energy (Cheah et al., 2017) or super-hydrophobic property (Kakunuri et al., 2017) and high mechanical strength ensuring

that they do not break easily (Lu et al., 2017). There are various nanomaterials that are being exploited for their adsorption property such as nano-TiO_2, CNTs, dendrimers and other carbonaceous nanomaterials. However the toxicity of nanomaterials is a rising area of concern, especially in the field of wastewater treatment as it directly or indirectly affects the ecosystem (Tan et al., 2015a). Metal nanomaterials including oxides are known to be toxic in nature. For example: when TiO_2 is taken in bulk it is non-toxic, however TiO_2 is known to cause haemolysis of erythrocytes as well as hemagglutination in human beings and additionally produces tremendous changes in the ecosystem at relatively lower concentrations. Similarly, metal oxide nanoparticles of higher concentrations of Fe_3O_4, ZnO and MgO are toxic to human as well as animal cells.(Tan et al., 2015a). Nano forms of zerovalent ions (ZVI) has been reported to be safe for human, but it displays toxic in aquatic environments. (Keller et al., 2012). Similarly, oxides such as ZnO, TiO_2 and MgO are all toxic in decreasing order of toxicity. Similarly, carbonaceous nanomaterials are known to be toxic as well (Tan et al., 2015a) Thus, to combat the toxicity of nanomaterials there arose the concept of nanotechnology using biomaterials grew rapidly.

A convenient method through which this can be achieved is by the use of the electrospinning as the biomaterial can easily be encapsulated in the form of a nanofiber. It has remarkable advantages over others in aspects of efficiency, continuity, repeatability and applicability. The thesis is based on the removal of dyes using Nano adsorbents made from biomaterials. The biomaterial chosen for the study is *Moringa oleifera* (MO) which has shown very high adsorption capacities in the removal of heavy metal ions as well as certain dye like Congo red (CR). (Patel and Vashi, 2012) (Soliman et al., 2019)(Vijayaraghavan and Shanthakumar, 2015)(Tie et al., 2015) The dye Congo red is known to be metabolized to benzidine which is both carcinogenic as well as mutagenic. Literature survey showed that *Moringa oleifera* has high affinity to adsorb Congo red compared to other biosorbents. However not many effective forms are present to deliver *Moringa oleifera* for the adsorption process and research is being done on the same. The following thesis focuses on delivering *Moringa oleifera* more effectively to tap its full potential and to ensure regeneration of adsorbent to maximum extent.

1.1 Objectives

The research objectives of the present work are as follows

- To synthesize *Moringa oleifera* (MO) encapsulated Sodium Alginate beads through drop-wise gravity method.
- To synthesize *Moringa oleifera* loaded PAN nanofibers through electrospinning technique.
- To characterize the synthesized beads and nanofibers using various analytical techniques such as FESEM (Field emission Scanning electron microscope), TEM (Transmission electron microscope), XRD (X-Ray Diffraction), XPS (X-ray photoelectron spectroscopy) and FTIR (Fourier Transform Infrared spectroscopy).
- To perform adsorption experiments, kinetic and isothermal studies using two different adsorbents namely *Moringa oleifera* encapsulated Sodium Alginate (Na Alg/MO) beads and Moringa oleifera loaded (PAN/MO) nanofibers
- To investigate the effect of pH on the adsorption properties of both Na Alg/MO beads and PAN/MO Nanofibers.
- To perform the reusability studies of both Na Alg/MO beads and PAN/MO Nanofibers to study the longevity of the adsorbents.

1.2 Significance of present study

The significance and the salient features of the present thesis has been summarized below

- In this work, *Moringa oleifera* was incorporated into sodium alginate to form Na Alg/MO beads. Henceforth, two different adsorbents i.e. one in the form of beads and other in the form of nanofibers was prepared.
- Similarly, a homogenous polymeric blend solution of PAN/MO was prepared through solvent homogenization method and electrospun to form PAN/MO Nanofibers.
- For the first time, a biosorbent of MO was engineered to form nanofibers through the simple electrospinning technique and utilized for the removal of toxic organic dye (Congo red).
- Further, the two different forms of the adsorbents have undergone several batch adsorption experiments i.e. effect of contact time, effect of pH and the effect different concentration of dyes.

- The adsorption performance of the adsorbents was compared in all aspects and analyzed.
- From the results, it was ascertained that the adsorptive performance of both beads and nanofibers are similar in some extent.
- However, considering the practical feasibility and the commercial aspects, the nanofibrous biosorbent (PAN/MO Nanofibers) which is in the form of a sheet can be scaled up according to the industrial suitability.
- The adsorption studies on the effect of pH gives the mechanism involved in the adsorption process.
- Reusability studies of the adsorbents corroborated the stability and long-term adsorption properties.

CHAPTER 2 LITERATURE REVIEW

2.1 Environmental pollution

The anthropogenic release of heavy metals such as Arsenic, Nickel, Copper, Mercury, Cobalt etc. and other toxic materials like dyes a, effluents from industries into water bodies like streams, lakes, rivers and oceans is responsible for the decline in clean water we have today. The release of wastewaters containing dyes can affect the photosynthetic activity in aquatic life because of the reduced light penetration and therefore their decontamination is essential. Furthermore, the more stringent regulations concerning effluents require diminishing of the dye content in the water or even banning of some dyes. Dyes usually have synthetic origin and also a complex aromatic molecular structure that is stable and difficult to biodegrade. Among the organic dyes, the azo are majorly used dyeing processes. However, many azo dyes have proven to be very dangerous for human life because when the nitrogen-nitrogen bridge is cleaved under reducing conditions, it leads to aromatic amines which have been proven as or are suspected to be carcinogenic. The dye's attribute of possessing colour is due to the presence of chromophores which are conjugated double bonds consisting of delocalized electrons. That attach themselves to chromogenic which are aromatic structures. The chromophore-chromogen structure exists with auxochromes is what makes for high bonding affinity of the dye and the consequent difficult removal of dyes. Dyes can be classified as follows based on structural or function groups and colour, as well as by ionic charge upon dissolution in aqueous solution. The dyes are categorized into ionic and non-ionic dyes. Non-ionic dyes can further be categorized into vat dyes and disperse dyes, and ionic dyes can be classified further into cationic (basic), and anionic dyes (reactive, direct and acidic). (Tan et al., 2015a)

It has been established that dyes may cause problems in water by several ways:

- The effect of dyes on aquatic flora and fauna can be persistent and its magnitude depends on the concentration of dye as well as contact time. (Bharathi and Ramesh, 2013)
- Dyes can be easily seen even when a small quantity is present in the water. The colour produced by dyes in water makes it aesthetically unpleasant and toxic. (Bharathi and Ramesh, 2013)

- The dyes do not allow sunlight to penetrate the water effectively and thus adversely affect the aquatic flora and fauna.
- Dyes are composed of many different and complex molecular structures which cannot be broken; making it difficult to treat.
- The dyes can react and hence deplete aquatic life of dissolved oxygen which is critical to them. The consumption of water containing such dyes poses a risk of wastewater-borne diseases, which directly affects the environment and human health. Various methods such as chemical precipitation, filtration using membranes, using oxidation processes, adsorption, electrochemical technologies can be employed for the removal of various heavy metal ions from wastewater or aqueous solution. However, these methods consume high amounts of energy and are not economical. Adsorption is a low cost, non -toxic method and also one of the most effective methods (Ghaedi et al., 2013) .

2.2 Adsorption in dye removal

Adsorption occurs when a gas or liquid solute assembles on the surface of a solid or a liquid and consequently there is the formation of a molecular or atomic film. Thus, there is an attachment of atoms, biomolecules or molecules of liquid, gas and dissolved solids to a surface creating a layer of the adsorbate which are gradually being accumulated on the surface of the adsorbent. Hence it is a surface phenomenon. The exact nature of the bond formed solely depends on the interacting species, but can be classified into two main categories:

1. Physisorption: The type of adsorption wherein adsorbate attaches to the surface of adsorbent through Van der Walls (weak intermolecular) interactions.
2. Chemisorption: The type of adsorption where a molecule adheres to the surface of the adsorbent through a chemical bond.

Adsorption takes place mainly on the vicinity of the pore structure or at particular places inside the particle walls. Because pores are generally tiny in size, the internal surface area is greater than the external area. The separation on the surface mainly occurs as properties like molecular weight, shape or polarity differ among the molecules and as a result some molecules adhere more to the surface than others. In many cases, the adsorbate is held strongly enough to allow complete removal of that component from the fluid. In addition, proper adsorption has the potential to produce a high-quality treated effluent (Momina et al., 2018). There are various adsorbents used and the efficiency of the adsorbent depends on the affinity to its adsorbate, economical aspect, toxicity, regenerative capacity and availability

and should not cause formation of waste/sludge (Momina et al., 2018). The most common commercially available adsorbents are activated carbon, ion-exchange materials, biosorbents, zeolite, bentonite clay, etc. various adsorbents such as activated carbon (Tan et al., 2015b), fly ash, bentonite clay and zeolites, mesoporous silica, nanostructures such as carbon nanotubes, nanodiamonds, dendrimers, graphene oxide, and magnetic nanomaterials have been adopted to remove dyes from aqueous solutions. (Gao et al., 2019)

However, there are few disadvantages of adsorption which need to be overcome to make it more effective.

The disadvantages are:

- Recovery of the product being tough and expensive.
- Adsorption capacity reducing as number of cycles increase.
- Adsorbent regeneration requires an external source such as steam or vacuum
- Relatively high cost
- Spent adsorbent may be perilous in nature
- Some contaminants may react with the adsorbent and lead to dangerous explosions.

For example, activated carbon became one of the most popular adsorbents for the removal of pollutants from wastewater among all the sorbent materials proposed as it demonstrated a very high adsorption capacity. Activated carbon, a widely used as in adsorbent in industrial processes and comprises of structure which is microporous with large surface area and homogeneous nature. (Buczek, 2016). Activated carbon prepared from low cost material, mahogany sawdust, is considerably efficient for removal of direct dyes Pure Direct Blue 2B and Direct Green B dyes (Malik, 2004) methylene blue (Geçgel et al., 2013), Malachite green, acid yellow, Remazol black B, Remazol yellow etc. However, activated carbon has several disadvantages, such as it is quite expensive, has a problem in regeneration (Tan et al., 2015a) and is non-selective and ineffective against disperse and vat dyes (Saratale et al., 2011)(Kyzas et al., 2013). Therefore, the alternatives to activated carbon as an adsorbent became a crucial topic of research. The search for a new adsorbent not only had to be non-toxic but also regenerable and of high adsorption capacity as well.

2.2.1 Bio-sorption

Bio-sorption is the adsorption of non-living substances that are inactive and origin is biological. Their mechanism of removal of dyes is by binding and attaching to the metal ions from aqueous solution and are thus capable of removing dyes, metal ions and other toxic substances (Gupta et al., 2013). There are many materials with adsorptive ability of inorganic origin such as clays (bentonites, kaolinites, etc.), or fruit and other agricultural wastes, seeds of different plants, activated carbons from several types of woods etc. The bio sorbents are of organic origin and are mostly very efficient and economical, and they can be treated further to increase effectiveness and reusability. Due to differences in the nature of the bio sorbents used and the conditions when the bio-sorption experiment is conducted, it is difficult to compare the efficiency of the bio sorbents for the removal of metal ions and dyes. Activated Carbon can be produced from various biomaterials such as coffee husk ,pine cone, mango peels, rice husk, coconut shell; *Imperata cylindrica* leaf; rubber seed coat; banana stalk , groundnut hulls, ackee apple (*Blighia sapida*) seeds ,oil palm fruit fibre etc. (Bello et al., 2017). Some bio-sorbents studied for the removal of heavy metals and dyes in polluted waters are prepared from different parts of the Moringa oleifera tree, though its most well-known for the use of its seeds as both bio sorbent and coagulant. Some of the other commonly used dyes are rice husk for adsorbing textile dyes (Safa and Bhatti, 2011), peanut hull for removing the dye Methylene Blue (Taha and El-Maghraby, 2016), Orange peels for adsorption of Remazol Blue (Mafra et al., 2013), banana and Orange peels for dyes Methylene Blue, Congo Red and Methyl violet (Annadurai et al., 2002)

The wastewater produced during the processing of fabrics and leathers varies in chemical composition such as salts, organics, sulphur compounds, nutrients and toxic substances. In physical treatment process, several factors affect the bio-sorption of dyes which include various physio-chemical parameters such as pH, temperature, particle size of biosorbent used, dose of biosorbent, contact time of biosorbent and adsorbate and initial dye concentration. These directly influence the quantum of dye biosorption.

Type of dyes	Name of dye	Biosorbents	Literature
Direct dyes	Direct Blue	using maize cob, citrus peel and rice husk (agricultural wastes) in aqueous solution	(Saroj et al., 2014)
	Direct Black 38	Papaya seeds	(Weber et al., 2013)
	Congo Red	Moringa oleifera	(Tie et al., 2015)(Vijayaraghavan and Shanthakumar, 2015)
Cationic dyes	Methylene Blue	Raw eucalyptus barks (EB)	(Afroze et al., 2016)
	Methylene Blue	Dragon fruit peels	(Mallampati et al., 2015)
	Methylene Blue	Peanut hulls	(Taha and El-Maghraby, 2016)
	Malachite green	Banana peels	(Dahiru et al., 2018)
Acidic dyes	Acid Blue 113	Abelmoschus esculentus seed as biosorbent in aqueous solution in batch mode	(Lee et al., 2015)
	Acid Red 183	Fungal strains	(Saroj et al., 2014)
Reactive dyes	Reactive Black 5 and Reactive Orange 16	Aquai stalks	(Cardoso et al., 2011)
	Reactive red	Yeast slurry	(de Castro et al., 2017)

Table 1 Classification of different types of dyes, biosorbents and its literature works

2.3 Nanotechnology in adsorption

Another advance in adsorption is the use of nanotechnology. Two important properties of an adsorbent are: surface area and structure. The nanofibers that are prepared by the electrospinning method have the properties of high specific surface area and high porosity with fine pores. Nanotechnology has a huge role to play in adsorption as with the help of nanotechnology, as it can control the surface area to volume ratio. Carbon nanotubes are used to adsorb dyes such as acridine orange, eosin bluish, ethidium bromide, Orange C, CNT nanocomposites. Nano diamond and nano-chitosan is used in the adsorption of basic dyes, metallic nanoparticles such as titanium dioxide, zero-valent iron, magnesium oxide are used for adsorption.

Toxicity of nanomaterials is however a huge concern despite the potential application in water remediation. Nanomaterials be it metals, oxides or magnetic nanoparticles toxic. Some metal oxides are especially toxic in the nano-form than in the bulk form such as TiO_2 which is a cause of haemolysis and hemagglutination of erythrocytes in humans. Additionally, it can impact physical changes of components of the aquatic ecosystem at lower concentrations. Thus researchers started finding out biomaterials which can be encapsulated in nano-forms to ensure the benefit of high surface areas of nanomaterials and good adsorption capacity, non-toxic nature of biosorbents. An effective way to encapsulate biosorbents is through electrospinning The electrospinning process has become a popular method due to its relative ease of use, adaptability, ability to fabricate fibers with diameters on the nanometre scale, lots of possibilities for surface functionalization with high surface area to volume or mass ratio, small inter-fibrous pore size and high porosity Electrospinning, an electrostatic fiber fabrication technique, uses electrostatic forces to generate ultrathin fibers from polymer solutions or melts in the range of 10-20 kV. The process of electrospinning is a major focus of attention in recent years not only due to its flexibility in spinning a wide variety of polymeric fibers but also due to its ability to produce ultrathin and continuous fibers on a scale of nanometers that is otherwise difficult to achieve by using any standard technologies. Electrospinning set up is very simple and consists of three major components such as high voltage supply, spinneret with syringe and grounded collector.

The electrospinning process comprises of a source powered by high voltage, a nozzle and a collector with aluminium foil. A potential difference is created between the nozzle and collector consequently stretching of the solution which creates a thin jet from polymeric solution to the collector. Simultaneously, the solvent evaporates and the ultrafine nanofibers formed are collected.

During the process of electrospinning, a polymer solution flows through the capillary tube and is held at the end. When it is powered by a high voltage, charge is uniformly distributed over the surface of droplet coming out of the nozzle. The droplet is now subjected to electrostatic forces i.e. electric charge induced on the liquid surface and Coulombic force due to external electric field. The electrostatic repulsion between charges on the surface and the external field results in the morphological change in the droplet from pendant to conical shape known as Taylor cone. When increasing voltage exceeds threshold point where repulsive electrostatic force dominates surface tension resulting in inversion of rounded tip and ejection of charged jet from Taylor cone. In the meantime, solvent present in polymer solution evaporates leaving behind the nanofibers on the metallic collector. Sometimes problem may occur that the tip of needle gets blocked due to hydrolysis, condensation and gelation of precursor solution resulting in fabrication of nonuniform fibers. The problem can be surpassed by changing precursor or by adding suitable catalyst to adjust hydrolysis or gelation rate (Malwal and Gopinath, 2016).

2.4 Research problem identification

The task of integrating biomaterials in nanotechnology will be fruitful as the material will be easy to source, low cost, non-toxic and biodegradable and with the help of nanotechnology can be delivered in effective forms. The biosorbent chosen in this study is moringa oleifera as although a lot of research of being done on its role in water remediation, the search is on for better and easier forms of delivering and regenerating it. An attempt that has been made to deliver it in a rather effective manner is through the use of beads. The beads that have been made are effective but further optimization can be made with respect to concentration of Moringa oleifera in it. Another possible way of delivering this biomaterial can be through fibers. Nowadays a lot of nanofibers have been made using electrospinning using inorganic materials and recently are being made using biomaterials as well. However, there have been

no reports on nanofibers using seed content of Moringa oleifera. Thus, the attempt is to prepare nanofibers with Moringa oleifera using electrospinning method.

For application purpose we have chosen the model dye to be Congo red as studies have revealed that Congo Red was efficiently removed by Moringa oleifera seed cake with a high adsorption capacity.(Tie et al., 2015) (Vijayaraghavan and Shanthakumar, 2015)Thus the thesis will explore two ways of delivering moringa oleifera for the adsorption of Congo Red. Moringa oleifera encapsulated seed cake and Moringa oleifera electrospun nanofibers

2.4.1 Congo red: In our present work, congo red (CR) dye was taken as model dye for photocatalytic experiments. CR dye is an organic dye, the sodium salt of 3,3′-([1,1′-biphenyl]4,4′-diyl)bis(4-aminonaphthalene-1-sulfonic acid. It is an azo dye characterized by two nitrogen to nitrogen double bonds (-N=N-) that are usually attached to benzene and naphthalene rings [41]. When it is used as photocatalyst, the azo bonds are oxidized by free hydroxyl radicals or holes or reduced by electrons. The cleavage of azo bonds eases the de-coloration of CR dye. It is used as pH indicator as it can change colour from blue to red at pH 3 to 5.2. The colour of azo dyes is determined by the number of azo bonds present and the nature of chromophores and auxochromes attached (Liu et al., 2005) So, when it is dissolved in water, it leads to formation of red colloidal solution. It finds use in molecular biology laboratories for staining purposes. It is highly noxious because of its carcinogenic component (i.e. benzidyne). It creates skin irritation and has dreadful effects on respiratory system and reproductive system of human body.

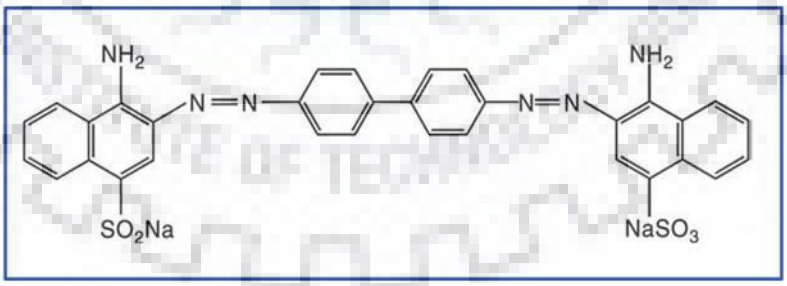

Figure 1 Molecular structure of CR dye

2.4.2 Moringa oleifera (MO): Moringa oleifera is a tropical plant that belongs to the Moringacae family. It exhibits properties of being non-toxic, an anti-oxidant and a natural organic polymer. It is known as a vegetable, for its medicinal properties. The leaves and young seeds of Moringa oleifera have ample quantity of Calcium, Iron and vitamin C. The seeds of Moringa contain water soluble proteins that are positively charged and thus behave

as a natural cationic polyelectrolyte. Thus the protein present in the Moringa binds to negatively charged particles. Studies done by Vieira et al. revealed that the use of Moringa oleifera shows high adsorption capacity and percentage removal of 98% for both colour and turbidity.(Vieira et al., 2012) The seed of moringa oleifera has been used in the removal of heavy metal ions mainly in the powdered form. The main concern of using the seed extracts is the residue matter that will be left behind after the treatment of water. Hence if we find a method to remove the adsorbed matter then the sludge generated will be non-toxic and biodegradable and can further be used as a fertilizer (Puyol et al., 2017). Thus, more effective forms for delivering moringa are being studied. Moringa oleifera encapsulated in alginate beads has been a recent experiment in which the beads were used to remove heavy metal ions such as copper, mercury and cadmium. It was found that the beads could remove over 90% of both the heavy metals(“Removal of heavy metals by natural adsorbent: review,” 2014). Similarly, the seed extract has ability to remove anionic dyes: azo, anthraquinones and indigoid dyes. (BeltránHeredia et al., 2009) However due to difficulty in separation of the seed components from the water, it is difficult to use.

CHAPTER 3 MATERIALS AND METHODS

3.1Materials Required

3.1.1 For synthesis of Na Alg/MO Beads

- **Sodium Alginate** (Mw = 199.65 g/mol), Alginate is a polyelectrolyte material that is commonly present in gel form. It can provide a relatively inert aqueous environment, encapsulate free of solvents, can control the porosity with single coating, which favours the formation of matrix for entrapment of both organic and inorganic compounds.
- **Calcium Chloride:** Calcium Chloride helps in hardening of beads by forming a crosslinked structure with Sodium Alginate.
- ***Moringa oleifera***: *Moringa oleifera* is the well-known species of the Moringaceae family. The plant is native to India but has spread all over the world, especially in tropical countries. Its seeds have been used for the treatment of turbid water due to their flocculation properties. The amino acids detected were mostly glutamic acid, proline, methionine and arginine. The leaves and seeds of Moringa oleifera are also widely used in water remediation as they have no significant side effect and are non-toxic and biodegradable (Ali et al., 2010) and have been used as biosorbents. Additionally, Research done by (Eman N. Ali, Suleyman A. Muyibi, Hamzah M. Salleh, 2009) on MO showed that coagulation activity is similar to the alum. The MO contain cationic polyelectrolytes which have proved to be effective in water treatment as an alternative for aluminium sulphate (Araújo et al., 2010). The flocculation activities of MO adsorb the metal cations based on the electrostatic charge mechanism (Suleyman A. Muyibi, and Megat, 2018)

3.1.2 Synthesis of PAN/MO Nanofibers

- **N, N- Dimethylformamide (DMF)** [C_3H_7NO] (Mw = 73.09 g/mol)
- **Polyacrylonitrile (PAN)** [$(C_3H_3N)n$] (Avg. Mw = 150,000)
- **M. oleifera** is the best-known species of the Moringaceae family. The plant is native to India but has spread all over the world, especially in tropical countries. Its seeds have been used for the treatment of turbid water due to their flocculation properties. The amino acids detected were mostly glutamic acid, proline, methionine and arginine. The leaves

and seeds of Moringa oleifera are also widely used in water remediation as they have no significant side effect and are non-toxic and biodegradable (Ali et al., 2010) and have been used as bio sorbents. Additionally, Research done by (Eman N. Ali, Suleyman A. Muyibi, Hamzah

M. Salleh, 2009) on MO showed that coagulation activity is similar to the alum. The MO contain cationic polyelectrolytes which have proved to be effective in water treatment as an alternative for aluminium sulphate (Araújo et al., 2010). The flocculation activities of MO adsorb the metal cations based on the electrostatic charge mechanism (Suleyman A. Muyibi, and Megat, 2018).

3.1.3 Adsorbate: Congo red (1-napthalensusulfonic acid, 3, 3-94,4-biphenylenebis (azo)) bis (4-amino) disodium salt) was supplied by Sigma. It is a carcinogen, mutagen and also very stable biologically owing to its complex aromatic structure. It is the sodium salt of benzidinediazo-bis-1-naphthylamine-4-sulfonic acid having a chemical formula C32H22N6Na2O6S2: and molecular mass: 696.66 g/mol was supplied by Sigma–Aldrich, India. The structure of Congo red molecule is as shown in Figure 1. The concentration of

CR in each aqueous solution was measured by the UV–vis spectrophotometer at λ_{max} = 500 nm.

3.1.4 Equipments used:

- Electrospinning machine (ESPIN NANO, PECO)
- Fourier transform infrared spectrometer (FTIR) (Thermo Nicolet)
- Transmission electron microscope (TEM) (JEOL 2100 UHR-TEM)
- UV–Visible spectrometer (Lasany double-beam L1 2800)
- X-ray diffractometer (XRD) (Bruker AXS D8 Advance)
- XPS (PHI 5000 VersaProbe III, Physical Electronics)

3.1.5 Synthesis of MO encapsulated Sodium Alginate beads:

The synthesis was done using the following steps

- 1 g of Moringa oleifera was taken in 50 mL of deionised water in a beaker.
- The above beaker was kept on a magnetic stirrer to ensure a homogeneous mixture is formed for a period of 24 h.
- 1g of Moringa oleifera seed powder was weighed and added to the above mixture.
- The above solution was then pipetted out drop-wise in a beaker containing 0.1 M $CaCl_2$ to form beads. This manner of forming beads is called "dropwise gravity method".
- The beads were then left to harden in a solution of 2 % $CaCl_2$ at 50 rpm for 24 h.
- After a period of 24 h, the hardened beads formed were filtered and air dried. Wet beads may be used as well however it has been shown that dry beads are more effective than wet beads.
- The hardened beads may be stored in any air tight container.

Figure 2 Synthesis of Sodium alginate/*Moringa oleifera* (Na Alg/MO) beads

3.1.6 Synthesis of Moringa oleifera incorporated PAN Nanofibers (PAN/MO):

- A solution of 7% PAN in 8 mL Dimethylformamide as solvent was prepared in the following manner
- 5 mL Dimethylformamide was taken in a vial and 560 mg PAN was added to it.
- 3 mL Dimethylformamide was taken in a falcon tube and 60 mg Moringa Oleifera was added to it.
- The solution in the falcon tube was further ultrasonicated to ensure uniform dispersion of Moringa Oleifera in the solution.
- The ultrasonicated solution is then added to the vial and is left for curing at a temperature of 80 °C for 3 h and fed into syringe for electrospinning.
- The fibers are obtained are stored for application purpose.

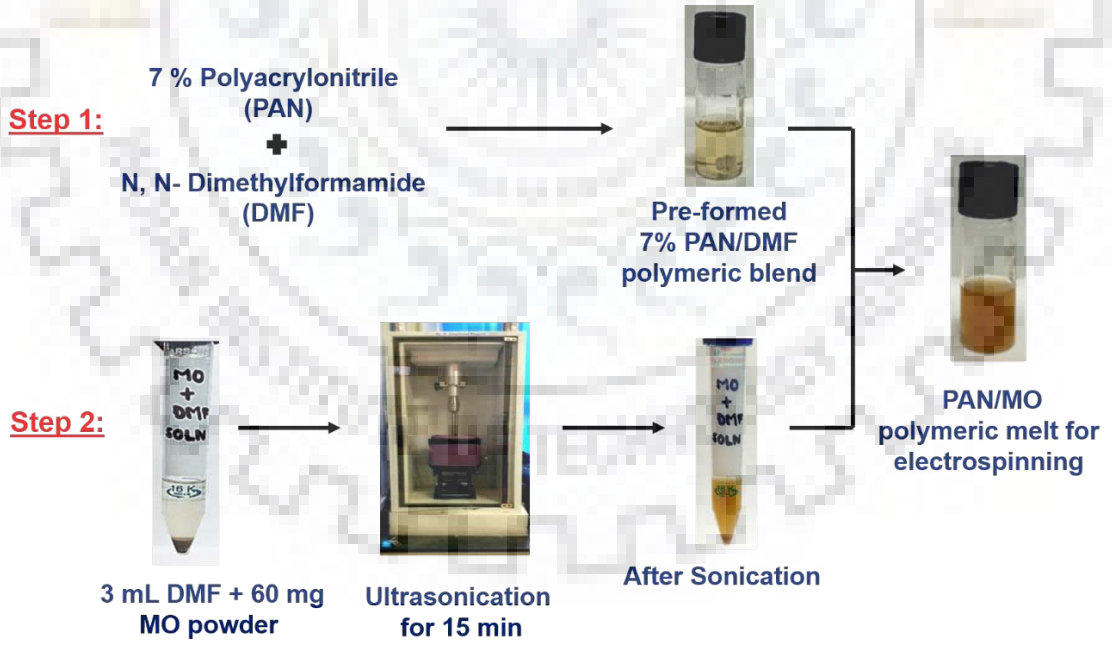

Figure 3 Fabrication procedure of PAN/MO polymeric blend

3.2Characterisation:

3.2.1 Field emission scanning electron microscopy (FESEM)

3.2.1.1 Na Alg/MO beads

The morphology of the Na Alg/MO beads was analyzed by Ultra plus-Carl Zeiss (Germany) field emission scanning electron microscope (FE-SEM) operated at 15 kV

3.2.1.2 PAN/MO nanofibers

The morphology of the PAN/MO nanofibers was analyzed by Ultra plus-Carl Zeiss (Germany) field emission scanning electron microscope (FE-SEM) operated at 15 kV

3.2.2 X-Ray Diffraction (XRD)

3.2.2.1 Na Alg/MO Beads:

The X-Ray diffraction was performed using Brucker AXS D8 advanced powder X-ray diffractometer with Cu-Kα radiation of wavelength λ = 1.5404Å in the range of 20° to 90° with a scan rate of 0.5°/min. The diffraction peaks were analyzed using PANalytical Expert Highscore Plus software for both Sodium Alginate beads and Sodium Alginate beads with *Moringa oleifera*

3.2.2.2 PAN/MO Fibers:

The X-Ray diffraction was performed using Brucker AXS D8 advanced powder X-ray diffractometer with Cu-Kα radiation of wavelength λ = 1.5404Å in the range of 20° to 90° with a scan rate of 0.5°/min. The diffraction peaks were analyzed using PANalytical Expert Highscore Plus software for both Sodium Alginate beads and Sodium Alginate beads with *Moringa oleifera*.

3.2.3 Fourier transform infrared (FTIR) spectroscopy:

3.2.3.1 Na Alg/MO Beads

FTIR spectroscopy of nanofibers was performed by properly mixing small number of samples with KBr pellets using Thermo Nicolet spectrometer in the range of 4000-400 cm-1.

3.2.3.2 PAN/MO nanofibers

FTIR spectroscopy of nanofibers was performed by properly mixing small number of samples with KBr pellets using Thermo Nicolet spectrometer in the range of 4000-400 cm-1.

3.2.4 Transmission electron microscopy (TEM):

The transmission electron micrographs and selected area electron diffraction (SAED) patterns were obtained using JEOL JEM-3200FS Field Emission Electron Microscope working at 200 keV with machine resolution of 0.4 nm. The samples were prepared by sonication and dispersed a couple of drops onto the nonglossy surface of carbon-coated copper grids.

3.2.5 X-Ray photoelectron spectroscopy (XPS)

3.2.5.1 Na Alg/MO Beads

The chemical & electronic states and composition of as prepared Sodium Alginate with Moringa oleifera beads as well as Sodium Alginate beads were studied by using X-ray photoelectron spectroscopy (XPS) by exposing the samples with X-ray beam (A1 1486 single X-ray beam) and the equipment possessing C_{10} gun with vacuum pressure of 3.75×10^{-14} to 3.75×10^{-10} torr with 20 min of time of detector acquisition. All the raw data obtained were plotted in Origin Pro 8.0 software.

3.2.5.2 PAN/MO nanofibers:

The chemical & electronic states and composition of as-prepared nanofibrous membranes of PAN loaded with *Moringa oleifera* as well as PAN nanofibers were studied by using X-ray photoelectron spectroscopy (XPS) by exposing the samples with X-ray beam (A1 1486 single X-ray beam) and the equipment possessing C10 gun with vacuum pressure of 3.75 x 10-14 to 3.75 x 10 -10 torr with 20 min of time of detector acquisition. All the raw data obtained were plotted in Origin Pro 8.0 software.

3.2.6 UV-Visible spectroscopy

The quantitative measurement of the absorbance of dye samples after adsorption process was measured by UV-Visible spectroscopy. The dye solution was scanned in the wavelength range of 200-800 nm. The reading was determined using spectrophotometer (Lasany double-beam L1 2800). The absorbance of dye solution was taken at characteristic wavelength (λ = 500 nm) at fixed interval time. The concentration of dye was calculated using calibration curve plotted between absorbance and known concentration of the dye.

3.3 Batch adsorption studies

3.3.1 Adsorption study with effect of time

3.3.1.1 Na Alg/MO Beads: Adsorption experiments were carried out in five 50ml conical flasks containing Congo red solutions of concentrations 15ppm, 30ppm, 45ppm, 60ppm and 85 ppm. The flasks were kept in a shaker agitator at rpm of 300. The experiment was conducted for a time period of 8hours. The experiments were carried out using 25 mg of prepared beads. The same amount was added to all the flasks. The samples were withdrawn at pre-determined time intervals and the Congo red concentration was analysed using a UV-vis spectrophotometer. The amount of Congo red adsorbed at any time t is calculated by the following equation. The kinetic studies were carried out where the equilibrium concentrations were found out. The dye removal percentage were calculated for both beads and fibers.

3.3.1.2 PAN/MO Nanofibers: Adsorption experiments were carried out in five 50 mL conical flasks containing Congo red solutions of concentrations varying from 15 to 85 mg/L. The flasks were kept in a shaker agitator at 300 rpm. The experiment was conducted for a time period of 8 h. The experiments were carried out using 20 mg of prepared fibers. The same amount was added to all the flasks. The samples were withdrawn at pre-determined time intervals and the Congo red concentration was analysed using a UV-vis spectrophotometer. The amount of Congo red adsorbed at any time t is calculated by the following equation. The kinetic studies were carried out where the equilibrium concentrations were found out. The dye removal percentage were calculated for both beads and fibers.

3.4 Adsorption studies with effect of pH:

3.4.1 Na Alg/MO Beads:

The effect of pH was observed over a range of 2 to 13 at four different pH 2, 4.5, 7, 11 and 13. In this experiment, Congo red solution of 45 mg/L concentration was used for study. The study was conducted using 25 mg of prepared beads. The beads were added and the readings were taken at time intervals

3.4.2PAN/MO nanofibers:

Similarly, effect of pH was investigated over a range of 3 to 13 at four different pH ranging from 2, 4.5, 7, 11 and 13. In this experiment, Congo red solution of 45 ppm concentration was used for study. The study was conducted using 20 mg of PAN/MO fibers. The fibers were added and the readings were taken at time intervals.

3.5 Kinetic studies:

3.5.1 Na Alg/MO Beads: Adsorption experiments were carried out in five 50ml conical flasks containing Congo red solutions of concentrations 15 to 85 mg/L. The flasks were kept in a shaker agitator at 300 rpm. The experiment was conducted for a time period of 8 h. The experiments were carried out using 25 mg of prepared beads. The same amount was added to all the flasks. The samples were withdrawn at pre-determined time intervals and the Congo red concentration was analysed using a UV-vis spectrophotometer. The amount of Congo red adsorbed at any time t is calculated by the following equation. The kinetic studies were carried out where the equilibrium concentrations were found out. The dye removal percentage were calculated for both beads and fibers.

3.5.2 PAN/MO Nanofibers: Adsorption experiments were carried out in five 50ml conical flasks containing Congo red solutions of concentrations 15 to 85 mg/L. The flasks were kept in a shaker agitator at 300 rpm. The experiment was conducted for a time period of 8hours. The experiments were carried out using 25 mg of prepared beads. The same amount was added to all the flasks. The samples were withdrawn at pre-determined time intervals and the Congo red concentration was analysed using a UV-vis spectrophotometer. The amount of Congo red adsorbed at any time t is calculated by the following equation. The kinetic studies were carried out where the equilibrium concentrations were found out. The dye removal percentage were calculated for both beads and nanofibers.

3.6 Isotherm studies: Isotherms are plots which the general purpose of isotherms is to measure and to investigate the mechanism of sorption whether it is monolayer or multilayer adsorption.

3.6.1 Langmuir isotherm:

The Langmuir isotherm was published by Langmuir in 1916 to describe the interaction of gases adsorbed onto solids. The empirical model assumes that adsorption at saturation is formed over a single layer and that adsorption can only occur at specific sites, which are all homogeneous, such that there are no interactions that are lateral and no steric hindrance among the adsorbed molecules or active sites of the adsorbent The isotherm is semi-empirical and it is derived from a kinetic mechanism which is based on certain assumptions:

- The gaseous molecules that are adsorbed and the adsorbent molecules exist in dynamic equilibrium with each other
- The adsorption occurs at certain sites and these certain sites are all equivalent ▪ The molecules that have been adsorbed do not interact with each other.
- Even at maximum adsorption, there is only a monolayer of adsorbed molecules formed on the adsorbent.

Based on these assumptions, the formulated equation is shown below.

$$\frac{C}{q_e} = \frac{C_e}{q_m} + \frac{1}{q_m K}$$

Further, the key characteristics of the isotherm are explained with the help of separation factor

$$R_L = \frac{1}{1+bQ_m}$$

R_L Values	Type of adsorption
$R_L>1$	Unfavourable
$R_L=1$	Linear
$0<R_L<1$	Favourable
$R_L=0$	Irreversible

Table 2 Type of adsorption and its standard R_L value

3.4.2 Freundlich isotherm:

The Freundlich isotherm was proposed by Freundlich in 1909 and represents how the quantity of adsorbed gas on unit mass of solid adsorbent varies with pressure. It can be expressed as

$$Q_e = K_f C_e * \frac{1}{n}$$

Where, q: adsorption capacity in mg/g

C: equilibrium concentration of adsorbate adsorbed on the adsorbent in mg/L

K_f: distribution coefficient and n is a correction factor

In linear form it can be written as,

$$\log Q_m = logK_f + \frac{1}{n} logC_e$$

Thus K_f, the slope is the value of $1/n$ and the intercept is equal to log K_d

The major disadvantage of Freundlich isotherm is that it does not define the maximum adsorption of a gas onto a solid. The 1/n value which is obtained from the Freundlich isotherm tells us how linear the adsorption is or in other words, the degree of curvature of isotherms in the concentration range tested. The 1/n value usually ranges from 0 to 1. A value of 1 implies that the type of adsorption of the adsorbate onto the adsorbent was the same across the entire concentration range of adsorbate tested. This is unusual and the value of 1/n ranging from 0 to 1 shows that as the concentration of the adsorbate increases for a same amount of adsorbent, the relative adsorption decreases. This generally occurs due to the saturation of active adsorbent sites.

3.7 Reusability studies:

Adsorption study for both beads and nanofibers was studied by taking 25 mg of respective adsorbents using Congo red solution of 45 mg/L for a period of seven days

CHAPTER 4 RESULTS AND DISCUSSION

4.1 Synthesis

4.1.1 Na Alg/MO Beads

The beads synthesised become hard after a period of 24 hours. Sodium alginate has a unique property of forming calcium alginate gel through ionotropic gelation with each Ca+2 ion attaches to two strands of alginate under simple and mild conditions. The beads have the capacity possible to encapsulate both macromolecular agents as well as low molecular weight agents. The moringa particles entrapped in the alginate gel bead are clearly visible.

Figure 4 Synthesized Na Alg/MO beads after CR dye adsorption

4.1.2 PAN/MO nanofibers

The fibers are synthesised using the electrospinning method. The optimum concentration was found to be 7% PAN polymer in 8 mL Dimethylformamide. PAN is used as it hydrophobic in nature DMF and due to its high tensile strength. *Moringa oleifera* (MO)/DMF mixture was ultrasonicated to ensure that it is uniformly dispersed.

4.2Characterization:

4.2.1 FESEM

4.2.1.1Na Alg/MO Beads: The beads made of Moringa were characterised using FE-SEM to determine its morphology. Figure 5(a) shows the presence of bead like structures. Figure 5(b) and 5(c) show the rough porous nature of the beads on higher magnifications. Figure 5(d) yet represents the bead structure externally.

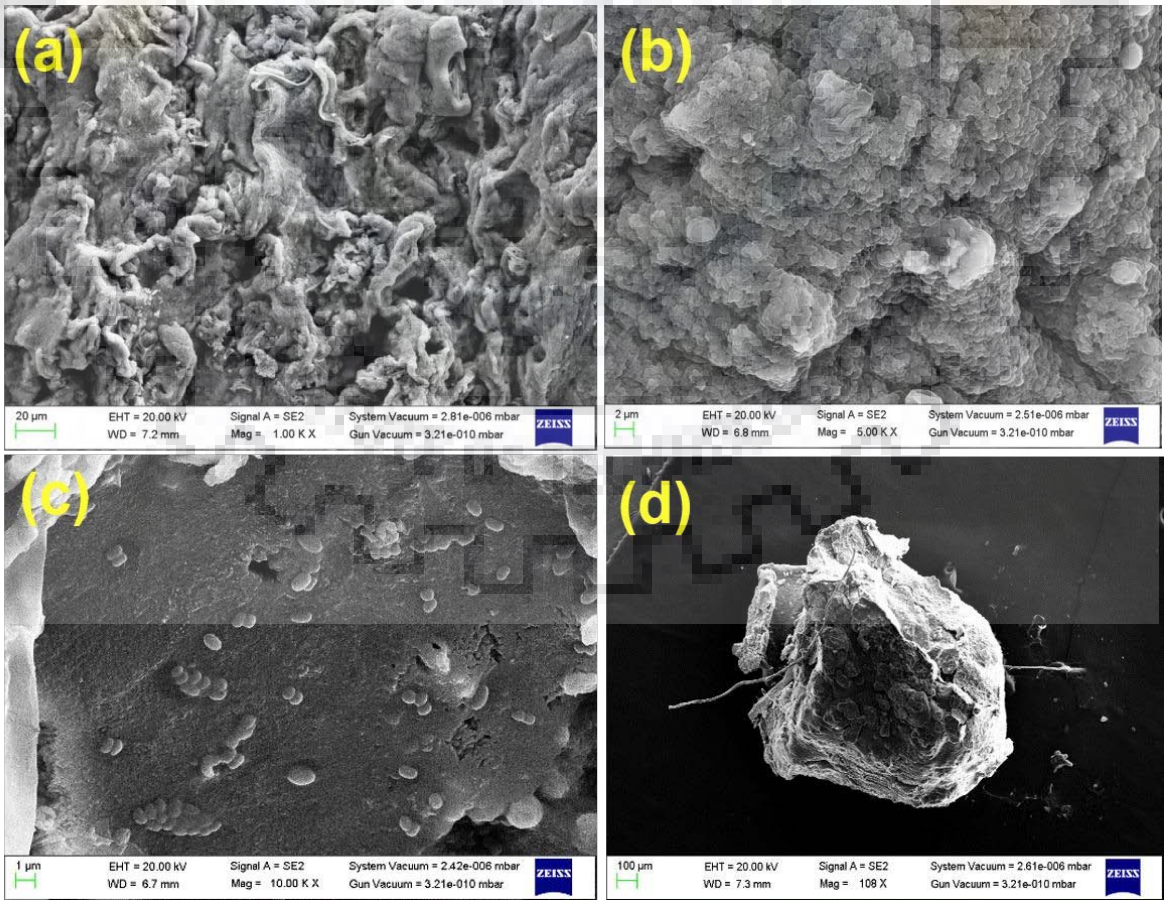

Figure 5 FESEM micrographs of Na Alg/MO beads (a-c) showing the magnified cross sections of beads and (d) at lower magnification (100 µm).

4.2.1.2 PAN/MO nanofibers: Figure 6a shows that the fibers are homogeneous and of uniform diameter. The diameter of the fibre was calculated using Image J software to be 96nm. Image C shows how the fibers give the appearance of being agglomerated at the Moringa oleifera particle. The EDX image confirms the presence of elements C, N, O and K.

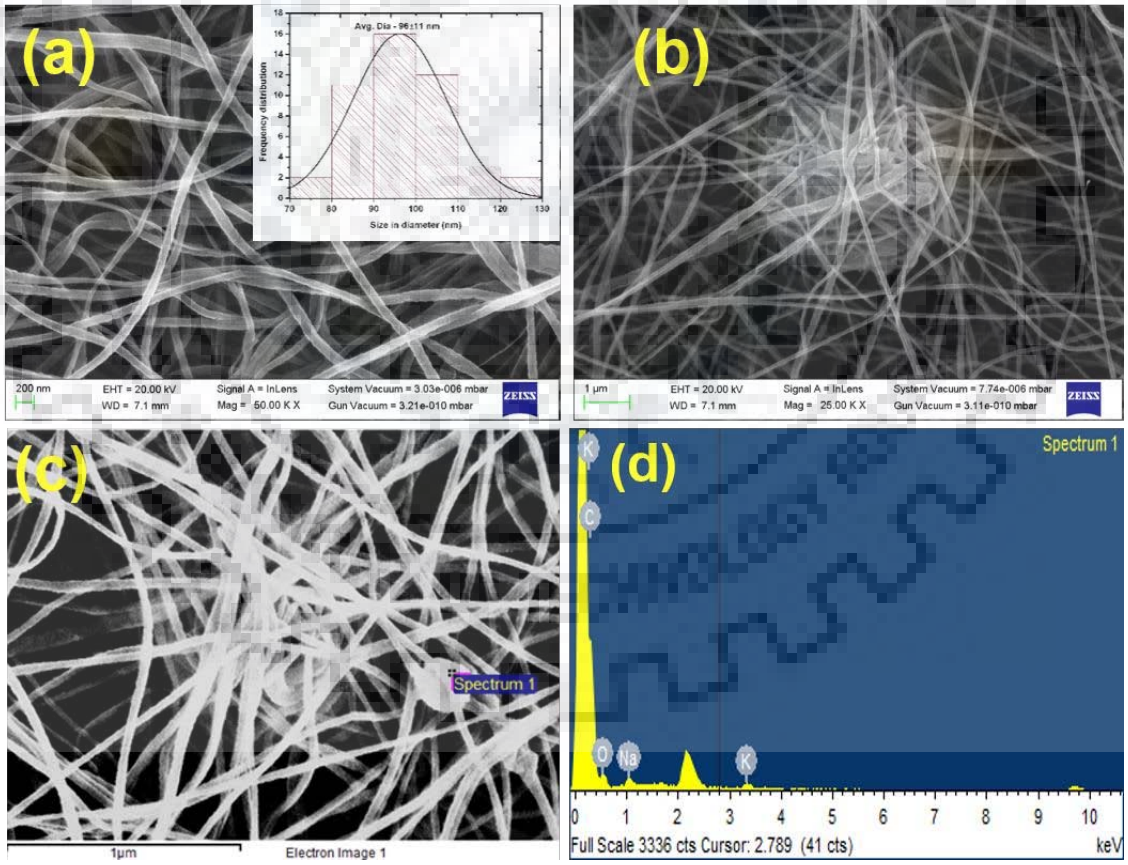

Figure 6 FESEM micrographs of PAN/MO nanofibers (a-c) at different magnifications. Inset showing size distribution and (d) EDX analysis.

4.2.2 TEM:

Figure 7a shows the presence of Moringa oleifera particles embedded along the vicinity of the fibers. Figure 7b taken at a resolution of 200 nm confirms the rough porous structure of the nanofibers. Inset of Figure 7b shows the presence of SAED pattern which confirms the amorphous nature of the fibers. Figure 7c is the EDAX analysis of the fibers which confirms the presence of elements Na, K and Mg which are all present in trace quantities in Moringa oleifera (MO).

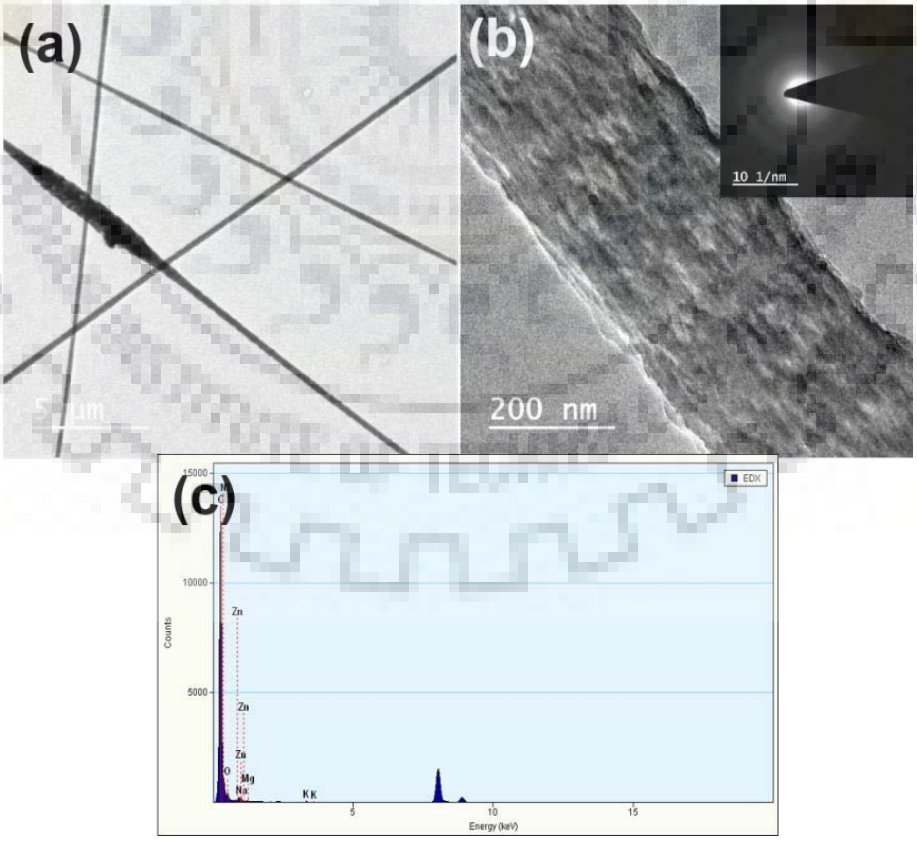

Figure 7 (a-c) TEM micrographs of (a) PAN/MO nanofibers (b) a single nanofiber and (c) EDX analysis

4.2.3FTIR

4.2.3.1 Na Alg/MO beads

The plot in Figure8(a) shows that sodium alginate has a peak centring at 3239.05 which is the result of stretching of hydroxyl groups. has characteristic peaks owing to stretching of carboxylate anions resulting in peaks centred at 2109.67, 1595.3 and 1412.66cm. The band centred at 1021.29 can be attributed to the pyranosyl ring of Sodium Alginate. In Figure8(b) the shift to 3419 is mainly due to the presence of amide groups of proteins, carbohydrates and fatty acids present in seeds additional to the stretching of hydroxyl bonds. Amines having the N-H bond and ketones that have C=C bond fill the spectrum from 1600-1800.

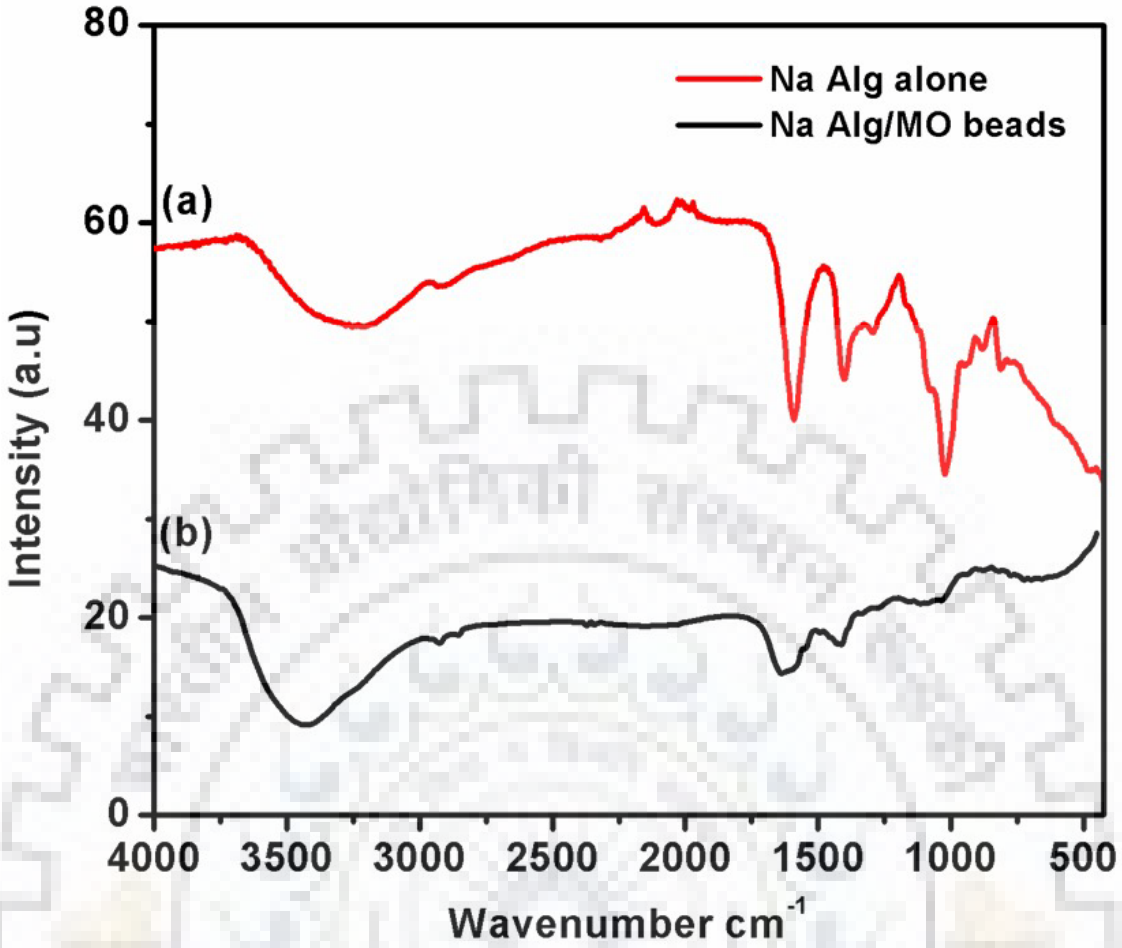

Figure 8 FTIR analysis of (a) Na Alg bead alone and (b) Na Alg/MO beads

4.2.3.2PAN/MO nanofibers

In Figure 9(a), The peak at 3431 signifies the O-H bond in PAN. The spectra shows peaks present at 2924.38 which is mainly due to the C-H bonds in PAN. The peak at 2238.73 is the classic peak of PAN which denotes the nitrile peak in PAN. The other peaks which are at 1591.29 is due to the amide groups which get shifted to 1627.10 due to the presence of other amide groups present in the insides of the seed. Similarly in (a) the peak at 1445.68 is due to the CH2 bonding whereas in Figure 9(b), there is a shifting at 1408.33.due to C=O bonding in phenols.

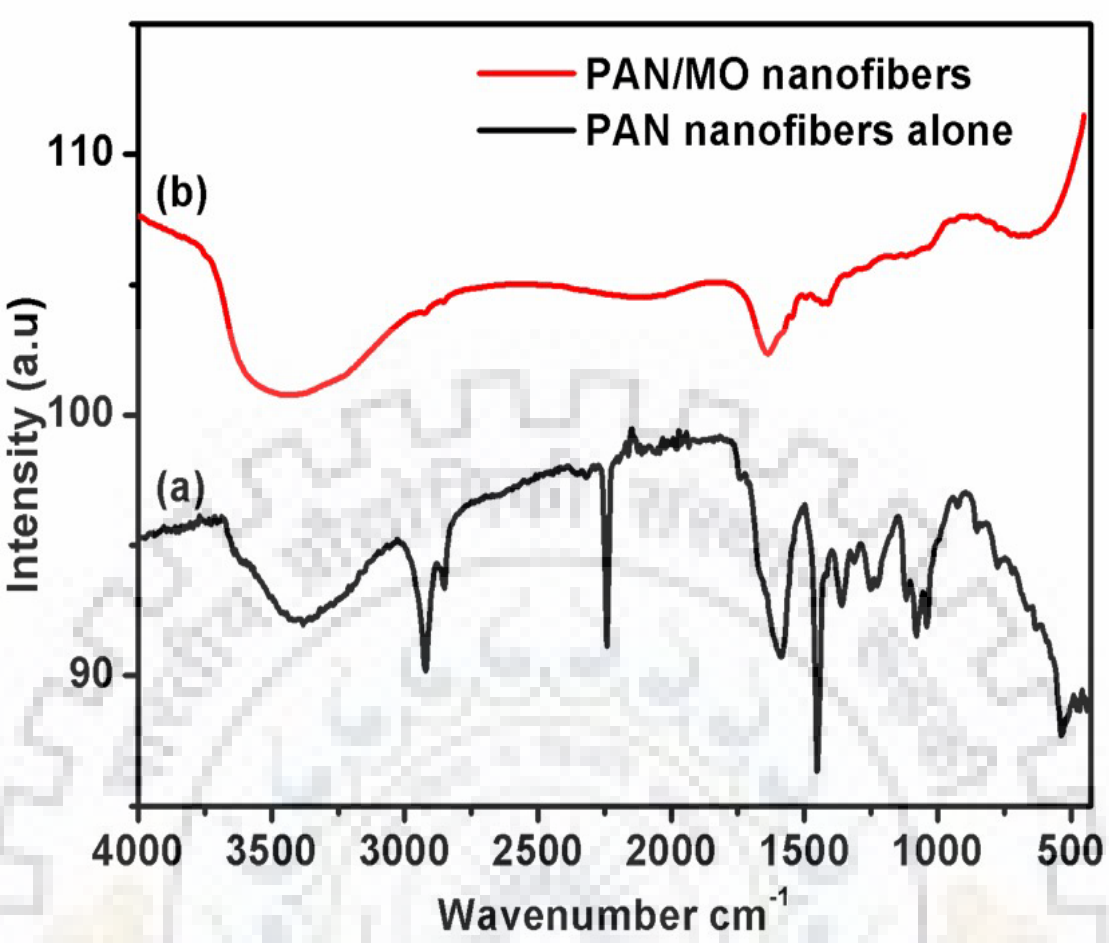

Figure 9 FTIR analysis of (a) PAN nanofibers alone and (b) PAN/MO nanofibers

4.2.4 XRD:

4.2.4.1 Na Alg/MO Beads

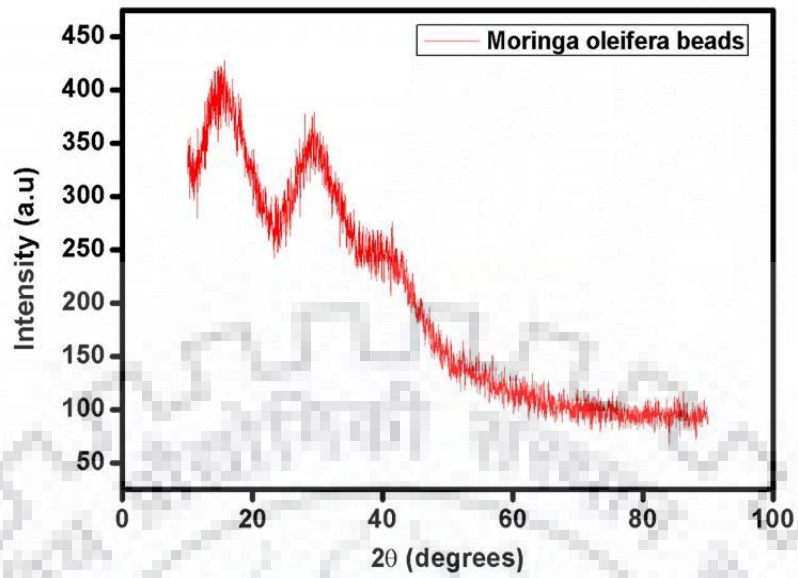

Figure 10 XRD spectra of Na Alg/MO beads **4.2.4.2**

PAN/MO Nanofibers

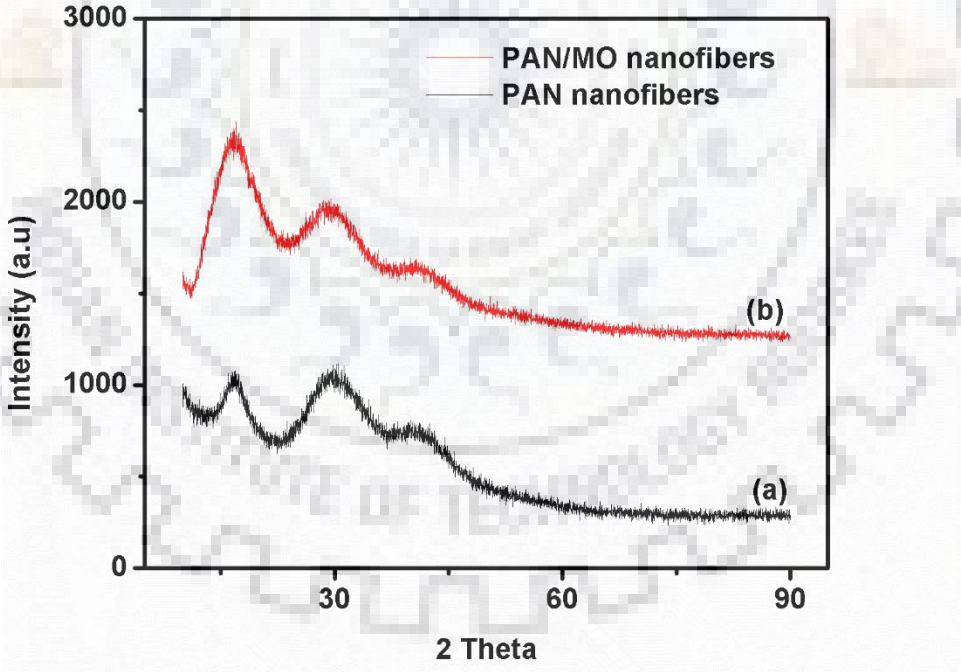

Figure 11 XRD spectra of (a) PAN nanofibers and (b) PAN/MO nanofibers

4.2.5 XPS

4.2.5.1 Na Alg/MO Beads: The full spectra illustrate the elements present in the bead after adsorption. The presence of Sulphur shows that adsorption of Congo red has occurred on the beads as the beads do not contain any sulphur in them. The other graphs show us the various energy states of the elements.

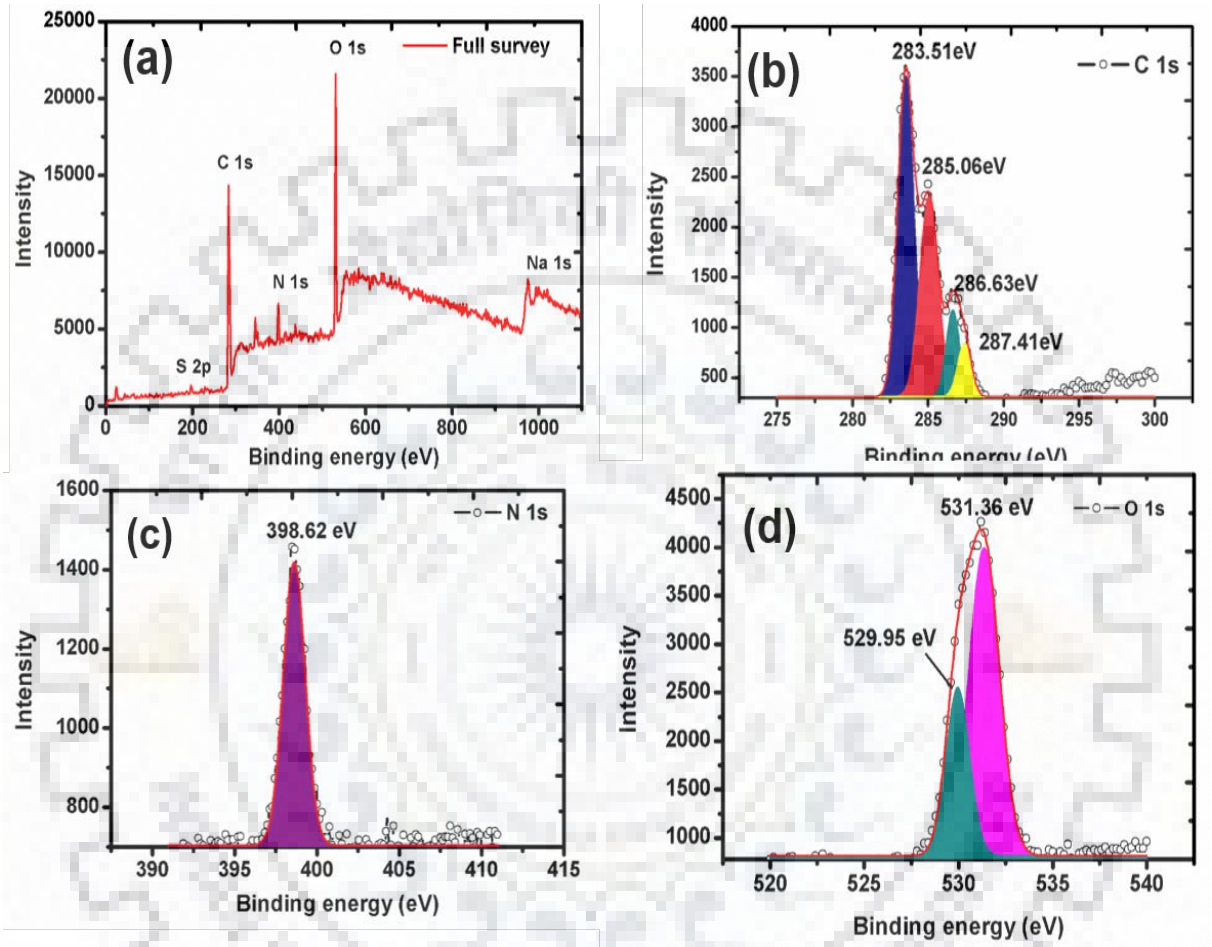

Figure 12 XPS analysis of Na Alg/MO beads showing (a) Full survey and De-convoluted spectrum of (b) C 1s, (c) N 1s and (d) O 1s.

4.2.5.2 PAN/MO Nanofibers

The full spectra illustrate the elements present in the bead after adsorption. The presence of Sulphur shows that adsorption of Congo Red has occurred on the fibers as the fibers before adsorption do not constitute of sulphur whereas the fibers after adsorption show the presence of Sulphur. The other graphs show us the various energy states of the elements

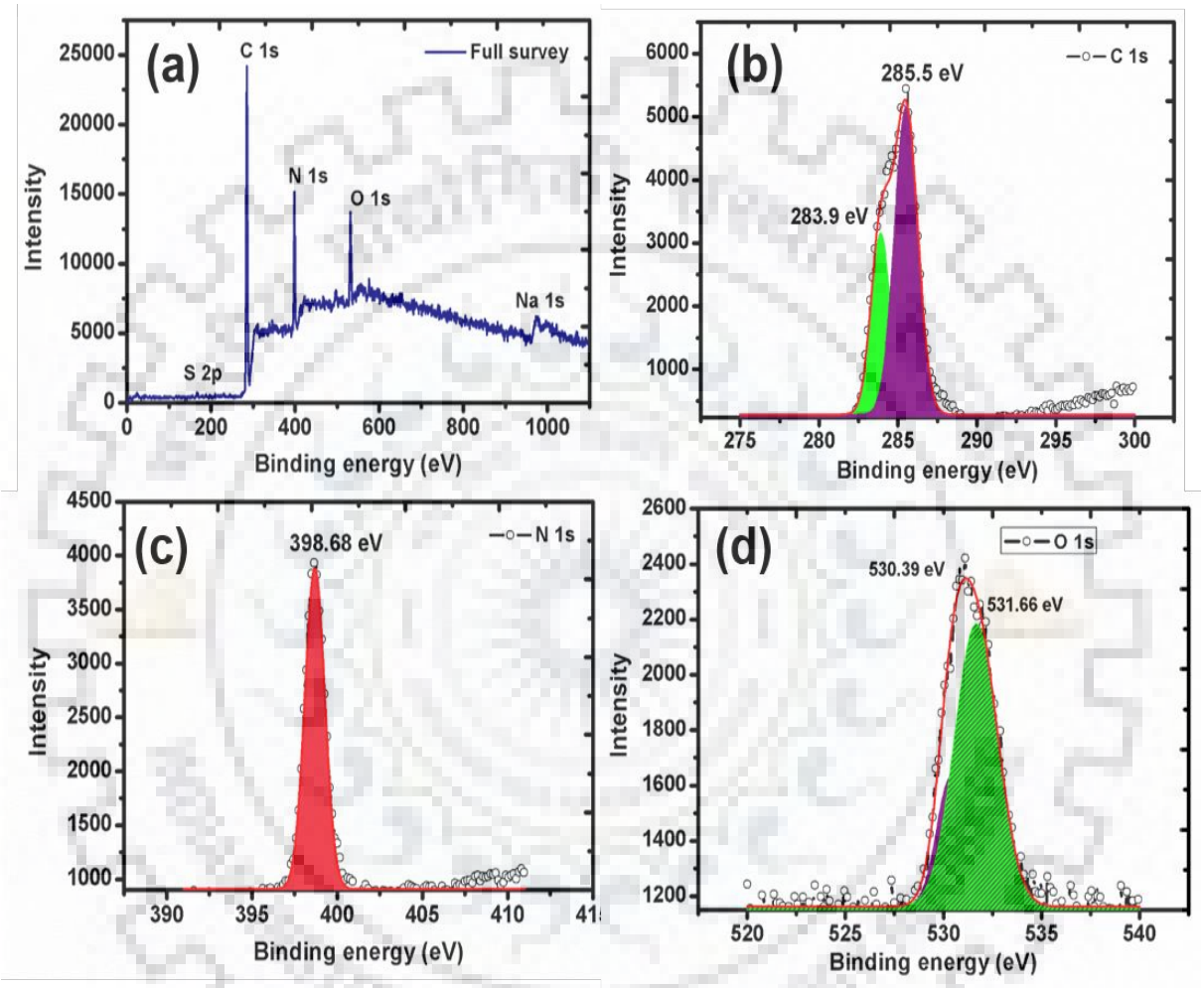

Figure 13 XPS analysis of PAN/MO fibers showing (a) Full survey and De-convoluted spectrum of (b) C 1s, (c) N 1s and (d) O 1s.

4.3Batch adsorption studies:

To study the adsorption properties of Na Alg/MO beads and PAN/MO nanofibers batch adsorption studies were performed using Congo red (CR) dye. The dye concentration was determined using UV-vis spectrophotometer (Lasany double beam LI-2800) from the calibration data reported earlier (Malwal and Gopinath 2015). Laboratory prepared CR dye solutions of varying concentrations from 15 mg L-1 to 85 mg L-1 with pH of ~7 until reaches the equilibrium adsorption and in specific, for performing the effect of pH studies, 45 mg/L of dye concentration was fixed as constant. The effect of adsorption time, effect of pH experiments was conducted batch wise for both type of adsorbents and the respective adsorption capacities were determined.

4.3.1Adsorption study- Adsorption capacity (qe) vs time

4.3.1.1 Na Alg/MO Beads The adsorption studies were conducted for five different concentrations such as 15, 30, 45, 60 and 85 mg/L in conical flasks with 25 mg of beads. Figure 14 shows the corresponding varying adsorption capacities of different concentrations of dye with time using Na Alg/MO beads and the data was represented in Table 3.

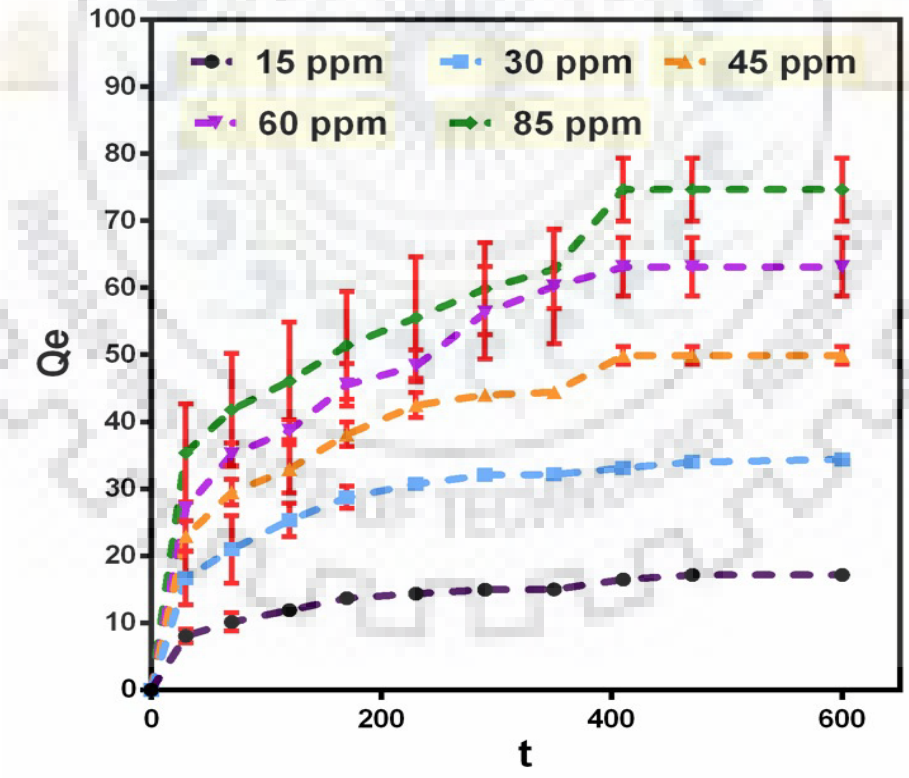

Figure 14 Time dependent adsorption study of Na Alg/MO beads showing adsorption capacity

versus time.

Concentration (mg/L)	15	30	45	60	85
Adsorption capacity (mg/g)	17.1909	34.7378	51.3810	67.9900	77.3924

Table 3 Representation of various adsorption capacities of the Na Alg/MO beads at different concentrations of CR dye

4.3.1.2 PAN/MO Nanofibers:

Simultaneously the adsorption studies with effect of time was conducted using PAN/MO nanofibers having same experimental conditions used for the beads. The graph showing different adsorption capacities with time using PAN/MO nanofibers was represented in Figure 15 and the respective data was tabulated (Table 4).

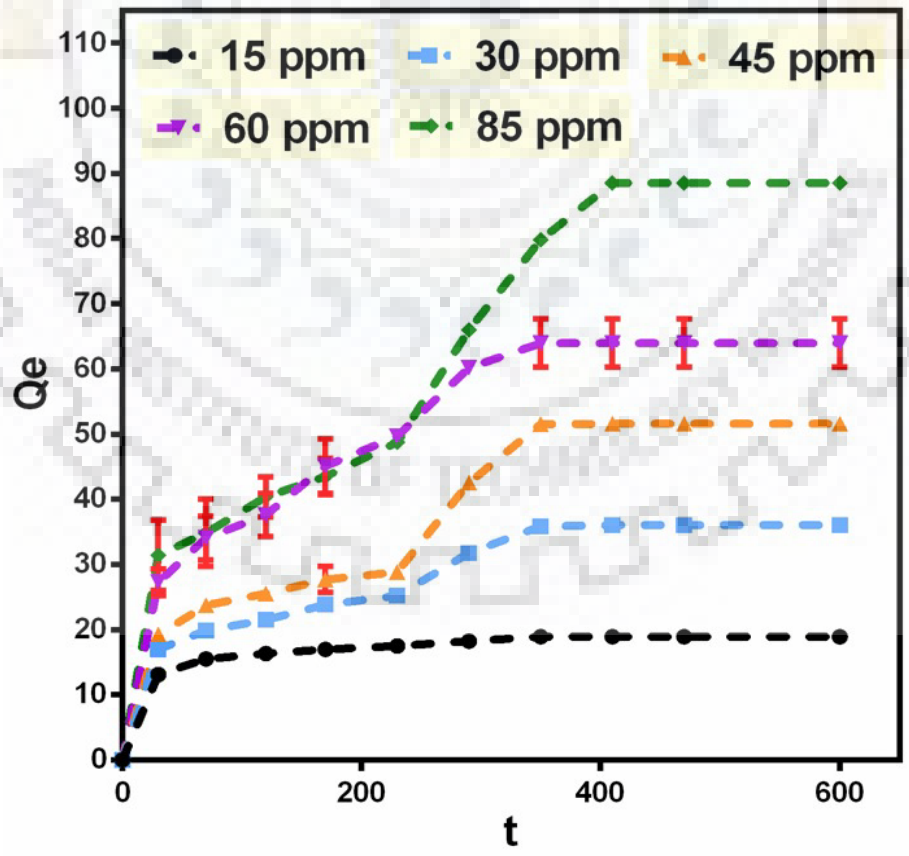

Figure 15 Time dependent adsorption study of PAN/MO beads showing adsorption capacity versus time

Concentration (mg/L)	15	30	45	60	85
Adsorption capacity (mg/g)	19.0053	35.9811	51.5692	68.2930	88.1854

Table 4 Representation of adsorption capacities of PAN/MO nanofibers at various concentrations of CR dye.

4.3.2 Adsorption studies: % Removal versus Concentration

4.3.2.1Na Alg/MO Beads

The following graph in Figure 16 shows the percentage dye removal versus different concentrations of dyes 15, 30, 45, 60 and 85 mg/L using the Na Alg/MO beads. The results show that the adsorption is higher in the case of lower concentration. However, as the concentration of the dye increased, the adsorption slightly decreased and attains equilibrium at some extended time. Hence, the average percentage removal can be observed to as ~80 %.

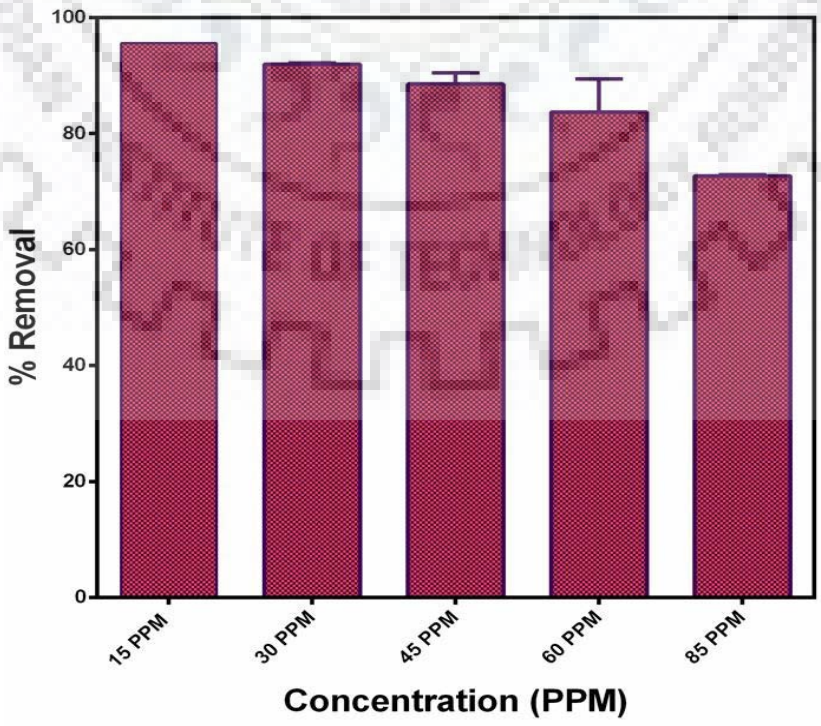

Figure 16 Adsorption study of Na Alg/MO beads representing the percentage removal with different CR dye concentrations

Concentration (mg/L)	15	30	45	60	85
% Removal	95.6602	90.1296	87.796222	82.89309	75.1060

Table 5 Representation of % Removal of CR dye at various concentrations using Na Alg/MO beads.From Table 5, it was inferred that the percentage removal of Congo red is higher for lower concentration and decreases as the concentration increases. The percentage removal of Congo red is greater than 80 percent across the concentration range and in specific greater than 90 % for 15, 30 and 45 mg/L.

4.3.2.2 PAN/MO Nanofibers

Similarly, the adsorption study of the PAN/MO Nanofibers with effect of contact time using different concentrations of CR dye followed the same trend of the beads. Figure 17 shows the % removal versus concentration plot showing decreased adsorption with increasing concentrations and the results are tabulated in Table 6.

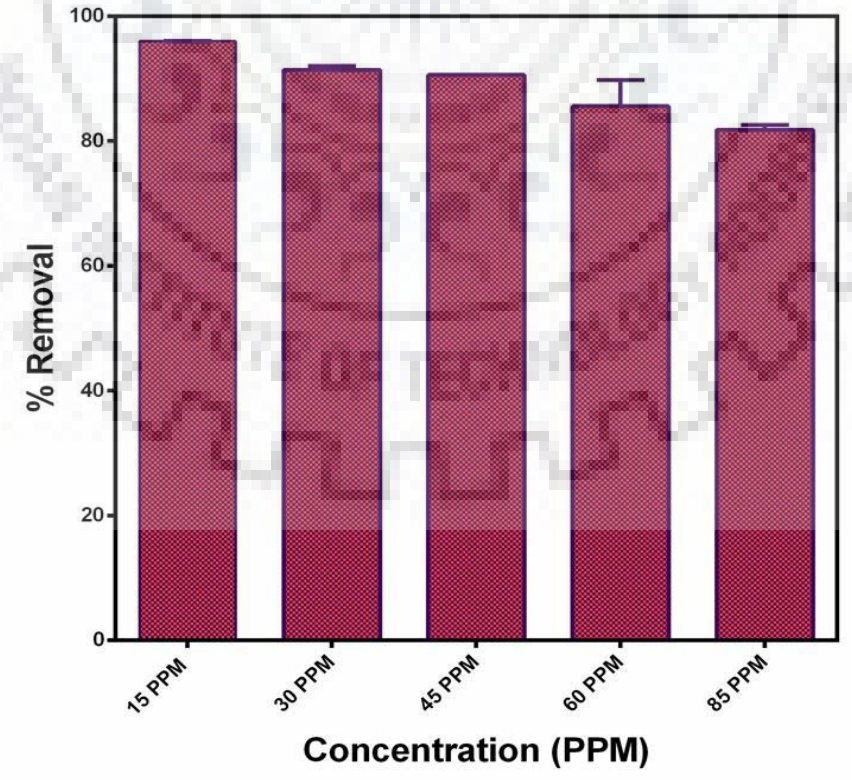

Figure 17 Adsorption study of PAN/MO nanofibers showing percentage removal with different CR dye concentrations

Concentration (mg/L)	15	30	45	60	85
% Removal	96.1702	91.0855	90.5962	84.8932	81.6651

Table 6 Representation of % Removal of CR dye at various concentrations using PAN/MO nanofibers.

4.4Adsorption study- Effect of pH

4.4.1 Na Alg/MO Beads: The variation in the adsorption properties was investigated by conducting adsorption experiments with the effect of pH. All the other experimental conditions were similar to the previously discussed studies except in which the dye concentration was kept constant as 45 mg/L. Figure 18 shows the adsorption capacities of Na Alg/MO beads with varying pH solutions with respect to time using uniform concentration (45 mg/L). Also the Table 7 represented the adsorption capacities for the corresponding pH.

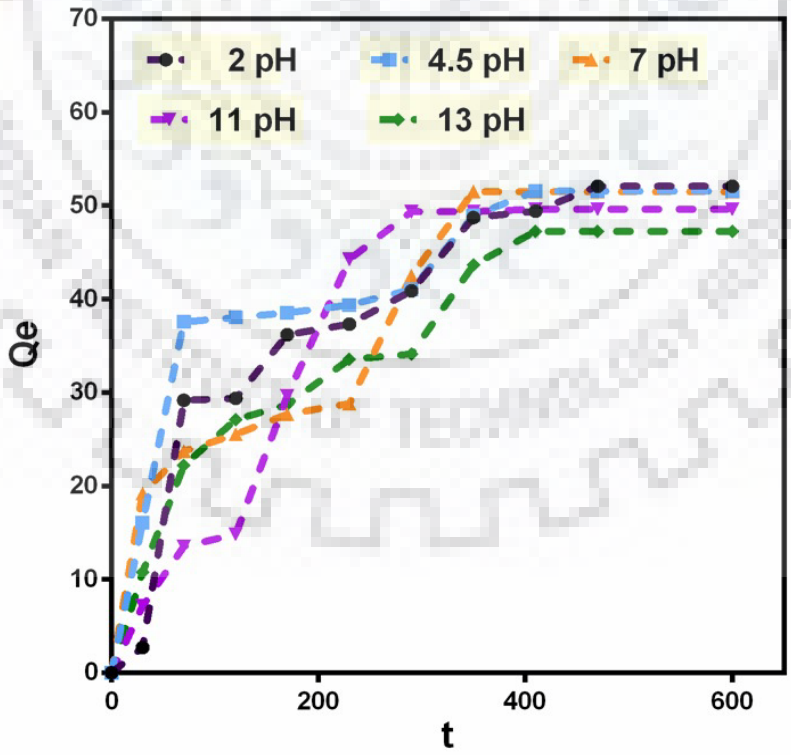

Figure 18 pH dependent adsorption study of Na Alg/MO beads showing adsorption capacity with time.

pH	**2**	**4.5**	**7**	**11**	**13**
Adsorption capacity Q_e (mg/g)	52.097	51.559	51.5	49.624	47.258

Table 7 Representation of adsorption capacities with different pH using Na Alg/MO beads.

Subsequently, the zeta potential of the different pH solutions and its adsorption capacity was shown in Table 7. From these results, it was ascertained that the adsorption capacity is higher in acidic conditions whereas the sorption capacity gradually decreases with increase in alkalinity. In addition, the pH profile for the Congo red sorption on biosorbent shows that dye sorption as a function of pH, exhibiting maximum sorption at lower pH (2.5), the sorbent is positively charged due to protonation of amino groups of the amino acids leading to electrostatic attraction between the biomaterial and anionic dye (Congo red). The results exhibit maximum sorption of Congo red (anionic dye) at low pH 2. Moreover, the graph shown in Figure 19 represented the % Removal of dye versus different concentrations of dye tranging from 15 mg/L to 85 mg/L.

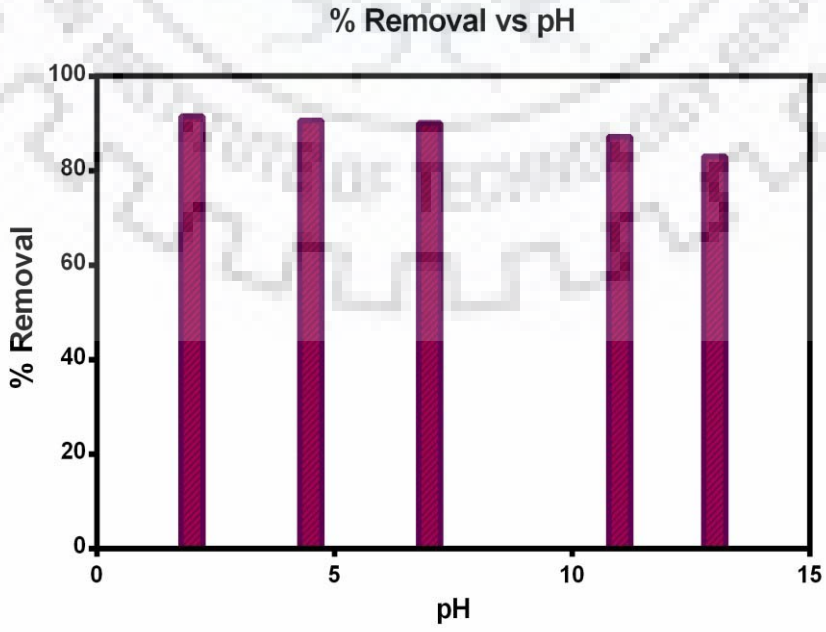

Figure 19 pH dependent adsorption study of Na Alg/MO beads representing % dye removal.

4.4.2 PAN/MO Nanofibers:

Similarly, the adsorption performance of the PAN/MO nanofibers with effect of pH was also studied by using the same experimental conditions as discussed in the case of Na Alg/MO beads. Figure 20 represented the pH dependent adsorption study PAN/MO nanofibers showing adsorption capacity with time t.

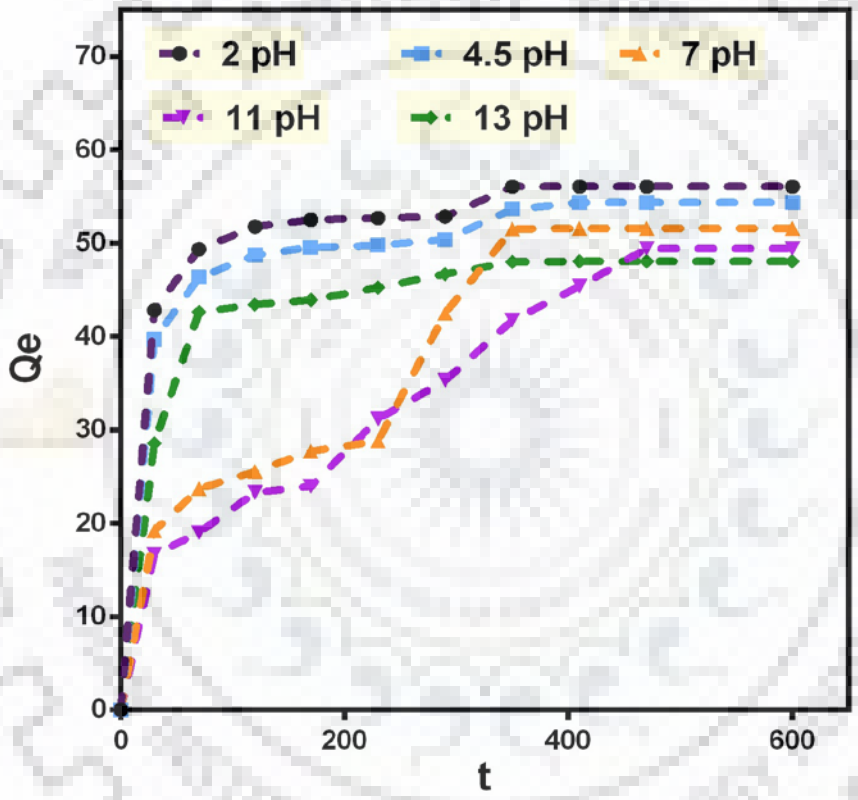

Figure 20 pH dependent adsorption study of PAN/MO nanofibers showing adsorption capacity with time t

pH	2	4.5	7	11	13
Adsorption capacity (mg/g)	56.062	54.337	51.569	49.409	48.065

Table 8 Representation of adsorption capacities with different pH of CR dye solutions using PAN/MO nanofibers.

From Table 8, higher adsorption capacity was observed in the case of acidic pH. But the sorption capoacity decreases as the aqueous solution gains alkalinity. Further, the corresponding percentage removal of CR dye with different pH was illustrated in Figure 21. Similarly, the PAN/MO nanofibers follows the similar trend of the adsorption capacities with the different pH of CR dye solutions having maximum sorption at lower pH (2).

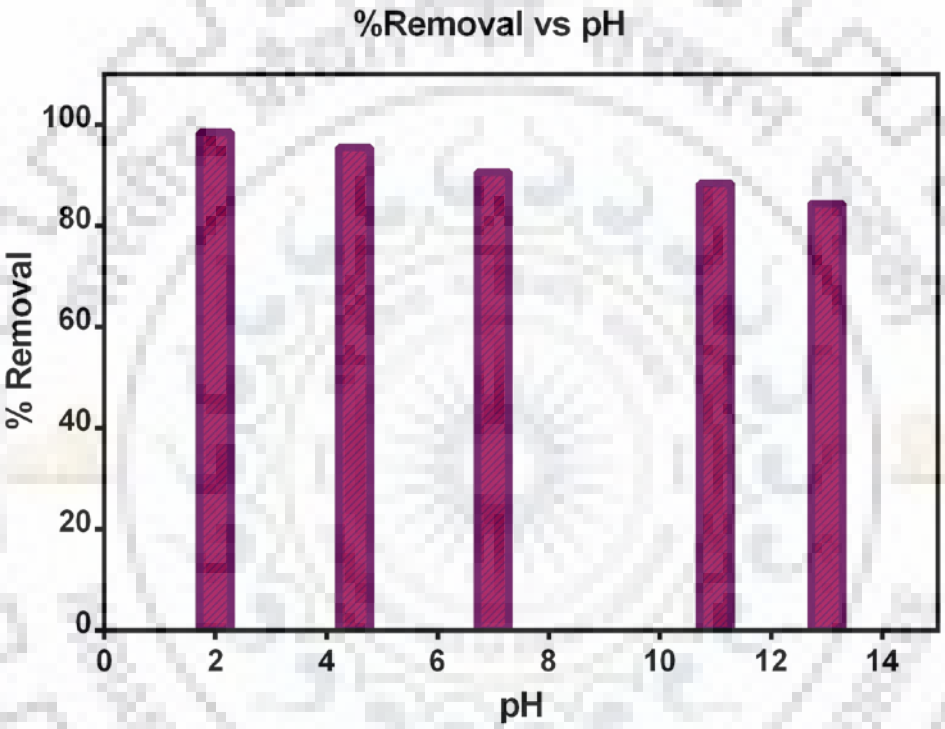

Figure 21 pH dependent adsorption study of PAN/MO nanofibers showing % dye removal versus time t

4.5 Kinetic studies:

4.5.1 Na Alg/MO Beads:

4.5.1.1 Pseudo first order is a plot between ln (Qe-Qt) vs t and the following table shows the parameters of the pseudo first order plot k and Qm

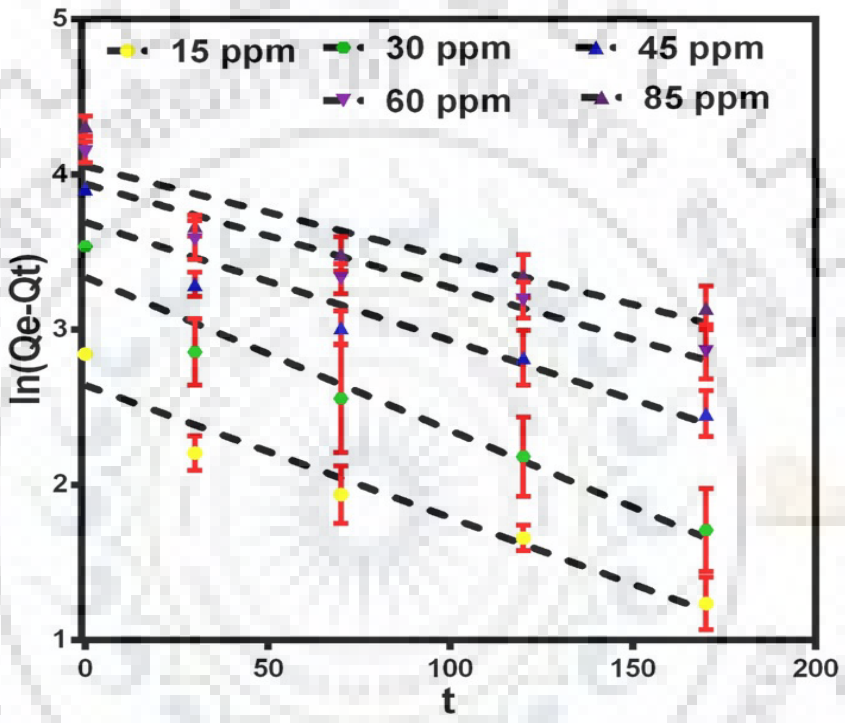

Figure 22 Pseudo-first order kinetic plot of Na Alg/MO beads

The above plot shown in Figure 22 represented the pseudo second order kinetics of PAN/MO nanofibers showing the graph between ln(Qe-Qt) vs t. The following table shows the parameters of the pseudo first order plot k and Qm that are calculated (Table 9).

Concentration (mg/L)	15	30	45	60	85
Slope (k)	0.0085	0.0098	0.0076	0.0066	0.0059
Q_m (mg/g)	16.7728	36.8324	48.9716	57.4712	60.3500
***R*2**	0.9053	0.8639	0.8777	0.8535	0.7853

Table 9 Kinetic parameters of pseudo-first order using Na Alg/MO beads.

4.5.1.2 Pseudo second order: Na Alg/MO Beads

Pseudo second order plot showing the graph between ln (Qe-Qt) vs t (Figure 23).

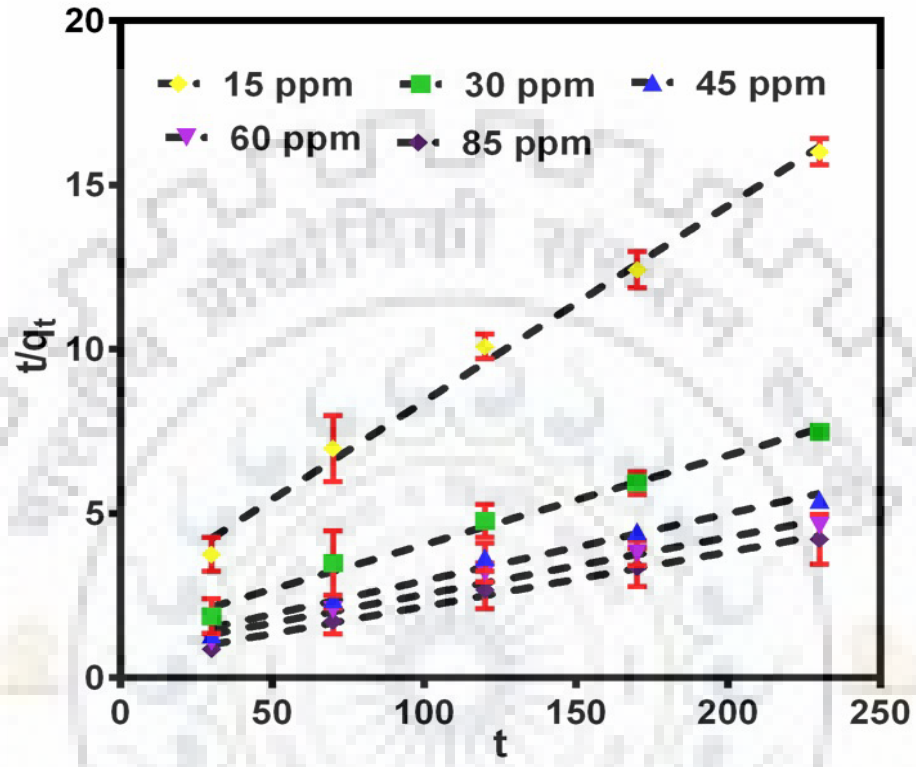

Figure 23 Pseudo-second order kinetic plot of Na Alg/MO beads

Concentration (mg/L)	15	30	45	60	85
Slope (K)	0.001424	0.00054	0.00045	0.0003767	0.00052
Q_m (mg/g)	14.069	28.219	40.2053	51.416	57.625
R_2	0.9792	0.9359	0.9630	0.9548	0.8714

Table 10 Representation of pseudo-second order kinetic parameters using Na Alg/MO beads.

From the pseudo first order plot, we can infer that the R^2 values are higher across the lower concentrations and is lesser for 85 mg/L.

Concentration (mg/L)	**15**	**30**	**45**	**60**	**85**
$Q_{m,\ exp}$	17.1909	34.7378	51.3810	67.9900	77.3924
Q_m (Pseudo-2nd Order	16.7728	36.8324	48.9716	57.4712	60.3500
Q_m (Pseudo 1st order)	14.069	28.219	40.2053	51.416	57.625

Table 11 Comparison of adsorption capacities ($Q_{m)}$ from both experimental and kinetic models using Na Alg/MO beads.

From the Table 11 and Table 12, it was inferred that the Q_m of theoretical and experimental are comparable for both pseudo first order as well as pseudo second order cases. Also, in both cases, the $Q_{m,\ exp} > Q_m$ (theory) for all concentrations of Congo Red. However, the values of $Q_{m,\ exp}$ of pseudo second order are more in agreement with Q_m theory as compared to Q_m pseudo first order.

Concentration (mg/L)	**15**	**30**	**45**	**60**	**85**
***R^2*(Pseudo-1st order)**	0.9053	0.8639	0.8777	0.8535	0.7853
***R^2*(Pseudo-2nd order)**	0.9792	0.9359	0.9630	0.9548	0.8714

Table 12 Comparison of correlation coefficients (R^2) from both experimental and kinetic model data using Na Alg/MO beads.

4.5.2 PAN/MO Nanofibers:

4.5.2.1 Pseudo-first order: This is the pseudo first order plot and it is a plot of ln (Q_e-Q_t) vs t (Figure 24). The following table shows the parameters of the pseudo first order plot k and Q_m.

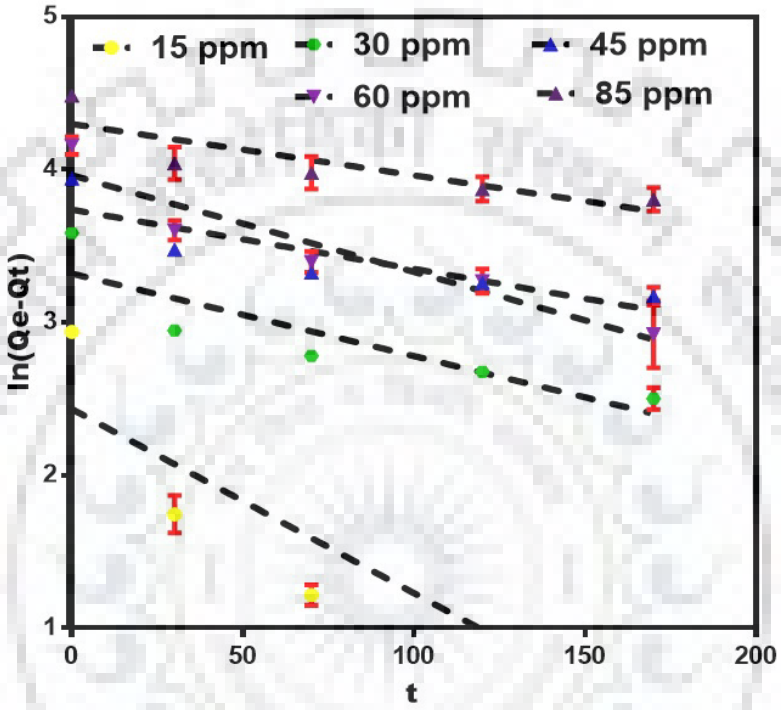

Figure 24 Pseudo-first order kinetic plot of PAN/MO nanofibers.

The following table shows the parameters of the pseudo first order plot k and Q_m that are calculated (Table 13).

Concentration (mg/L)	15	30	45	60	85
k	0.01205	0.005393	0.003876	0.006321	0.003361
Q_m (pseudo-first order)	11.4044	27.6327	42.0138	52.6149	73.6261
R_2	0.8158	0.7785	0.7478	0.8491	0.6877

Table 13 Representation of pseudo-first order kinetic parameters using PAN/MO nanofibers

4.5.2.2 Pseudo-second order

Pseudo second order plot showing the graph between ln (Qe-Qt) vs t (Figure 25).

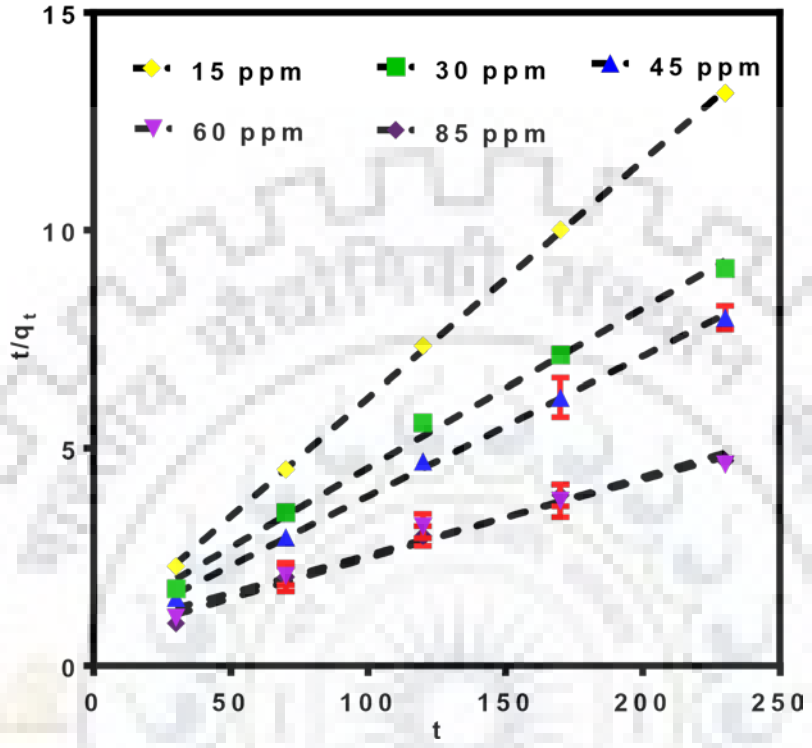

Figure 25 Pseudo-second order kinetic plot of PAN/MO nanofibers

Concentration (mg/L)	15	30	45	60	85
k	0.000412	0.00014	0.001466	0.00037	0.00055
Q_m (pseudo-second order)	18.3857	27.3822	31.2207	57.4712	58.8503
R^2	0.9989	0.9928	0.9912	0.9548	0.9665

Table 14 Representation of pseudo-second order kinetic parameters using PAN/MO nanofibers

Concentration (mg/L)	15	30	45	60	85
$Q_{m, exp}$	18.7290	35.9680	51.5690	65.2930	88.1855
Q_m (Pseudo-1st order)	11.4044	27.6327	42.0138	52.6149	73.6261
Q_m (Pseudo-2nd order)	18.3857	27.3822	31.2207	57.4712	58.8503

Table 15 Comparison of adsorption capacities ($Q_{m)}$ from both experimental and kinetic model data using PAN/MO nanofibers.

From Table 15 and Table 16, it was observed that $Q_{m, exp} > Q_m$ (theory) for all concentrations of Congo Red. However, the values of $Q_{m, exp}$ of pseudo second order are more in agreement for concentrations of Congo Red corresponding to 15 ppm and 30 ppm while $Q_{m, exp}$ of pseudo first order are more in agreement for the higher concentrations 45 ppm, 60 ppm and 85 ppm. Thus it becomes critical to compare the kinetics of the performance of fibers using the R^2 value.

Concentration (mg/L)	15	30	45	60	85
R^2(Pseudo-1st order)	0.8158	0.7785	0.7478	0.8491	0.6877
R^2(Pseudo-2nd order)	0.9989	0.9928	0.9912	0.9548	0.9665

Table 16 Comparison of adsorption capacities ($Q_{m)}$ from both experimental and kinetic model data using PAN/MO nanofibers.

From the R^2 values we can infer that the pseudo second order model is the appropriate model to describe the kinetics of the adsorption of Congo red dye by Moringa oleifera beads. In a nutshell, the experimentally processed adsorption data obtained from experiments conducted

on both adsorbents were validated using kinetic models such as pseudo-first order, pseudo second order. When the kinetic models were applied, the correlation coefficient values (R^2) obtained through pseudo second-order are very close to 1 compared to the values of first-order kinetics (Table 12 and Table 16).

4.6 Isothermal studies:

4.6.1 Na Alg/MO beads

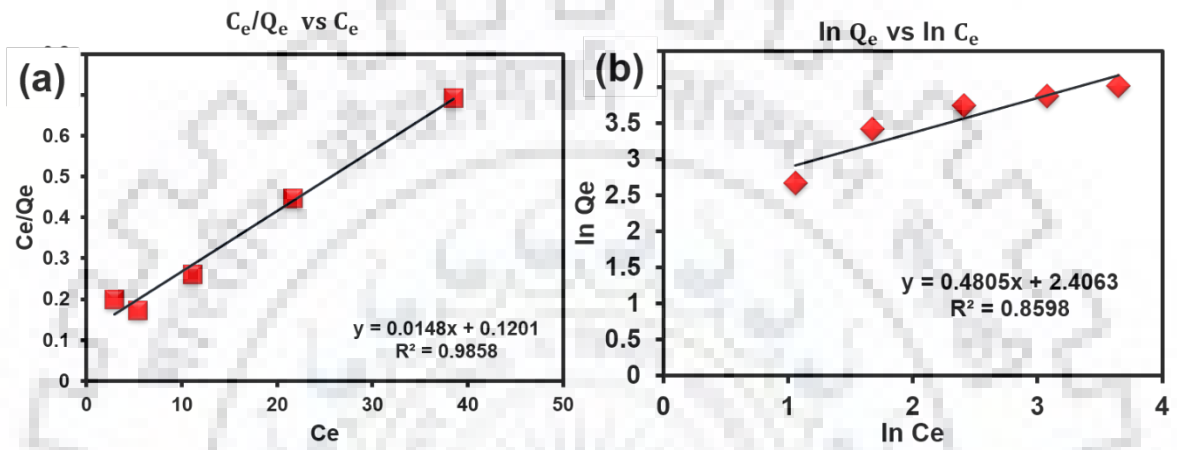

Figure 26 Isothermal plots of Na Alg/MO beads (a) Langmuir and (b) Freundlich models

4.6.2 PAN/MO Nanofibers:

The plot of C_e/Q_e vs C_e was plotted for the five different concentrations (Figure 27). Depending on the values the plot is made and the R^2 value was calculated. The various parameters such as theoretical maximum capacity and separation factor was calculated.

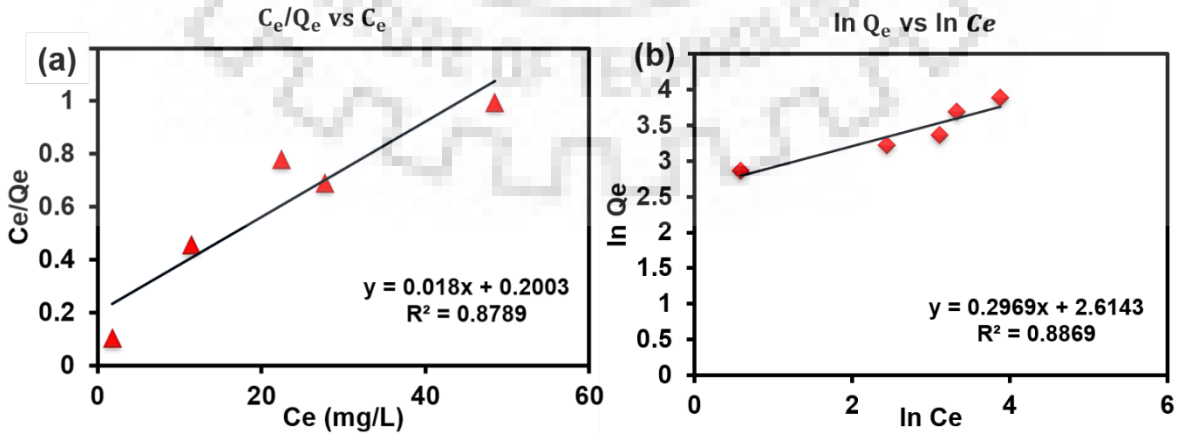

Figure 27 Isothermal plots of PAN/MO nanofibers (a) Langmuir and (b) Freundlich models

Sample	Q_m (mg/g)	K_L	R_L					R^2
Na Alg/MO beads	67.56	0.123	0.3511	0.2129	0.1528	0.1191	0.087	0.9858
PAN/MO Fibers	55.55	0.089	0.426	0.2712	0.1987	0.1568	0.116	0.8789

Table 17 Langmuir parameters of Na Alg/MO beads and PAN/MO nanofibers.

Samples	n	K_L	R^2
Na Alg/MO beads	2.08	11.09	0.8598
PAN/MO Nanofibers	3.368	13.657	0.8869

Table 18 Freundlich parameters of Na Alg/MO beads and PAN/MO nanofibers.

Comprehensively, the adsorption data obtained was fitted using empirical equations Langmuir and Freundlich isotherm models to determine the mechanism. Isothermal graphs of Langmuir and Freundlich are represented in Figure 26 and Figure 27. The isothermal parameters determined were represented in Table 17 and Table 18. From the above results it was observed that the correlation coefficients (R^2) of Langmuir shows better fit in comparison with the correlation coefficient values of Freundlich model in the case of Na Alg/MO beads.

Hence there is monolayer adsorption takes place in the beads. Conversely there is a possibility of both monolayer and multilayer adsorption to be occurred in case of the PAN/MO nanofibers due to the less significant R^2 values of Langmuir and Freundlich model. Additionally, the characteristic feature of Langmuir isotherm can be expressed by Langmuir constant, K_L was observed to be greater (i.e. 0.128 for beads and 0.089 for nanofibers) suggesting the higher affinity of CR dye onto both of the adsorbents. In the meanwhile, model parameters of Langmuir isotherm having the maximum adsorption capacity (Q_m) of 67.56 and 55.56 mg g^{-1} whereas the adsorption capacity (K_F) of Freundlich isotherm are 11 and 13.26 mg g^{-1} having 1/n value greater than 1 (i.e. 1.6409) suggested that the adsorption of dye onto the membrane is more Langmuir-like in Na Alg/MO beads and the combination of both models in the case of PAN/MO nanofibers. These findings necessitated the exploration of sorption property of the adsorbents towards the anionic dye.

4.7 Reusability studies:

The adsorptive property of the adsorbents was tested in a rational approach by the sequential adsorption-desorption process for minimum of five times. In brief, 25 mg of the adsorbent was used in each flask having same concentration of CR dye and the left dye concentration was measured after each adsorption cycle and the adsorbents were treated with 0.01 mol L^{-1} of NaOH simultaneously for desorption and air dried for the successive reusability studies. Histogram plot shown in Figure 20 and Figure 21 represented the regenerative property of the adsorbents by conducting the successive adsorption-desorption cycles which necessitated the industrial applicability of both the types of adsorbents.

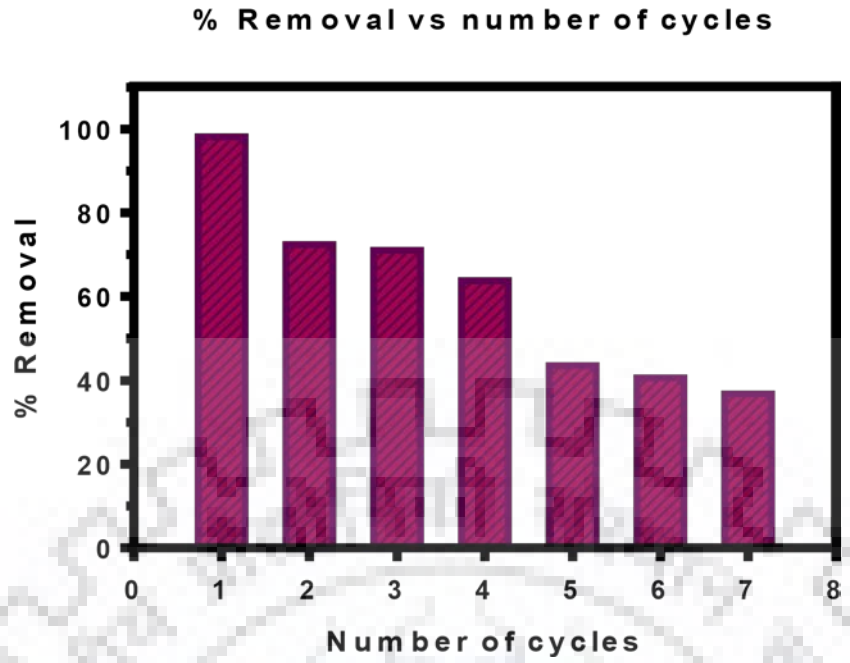

Figure 28 Reusability studies of Na Alg/MO beads using CR dye

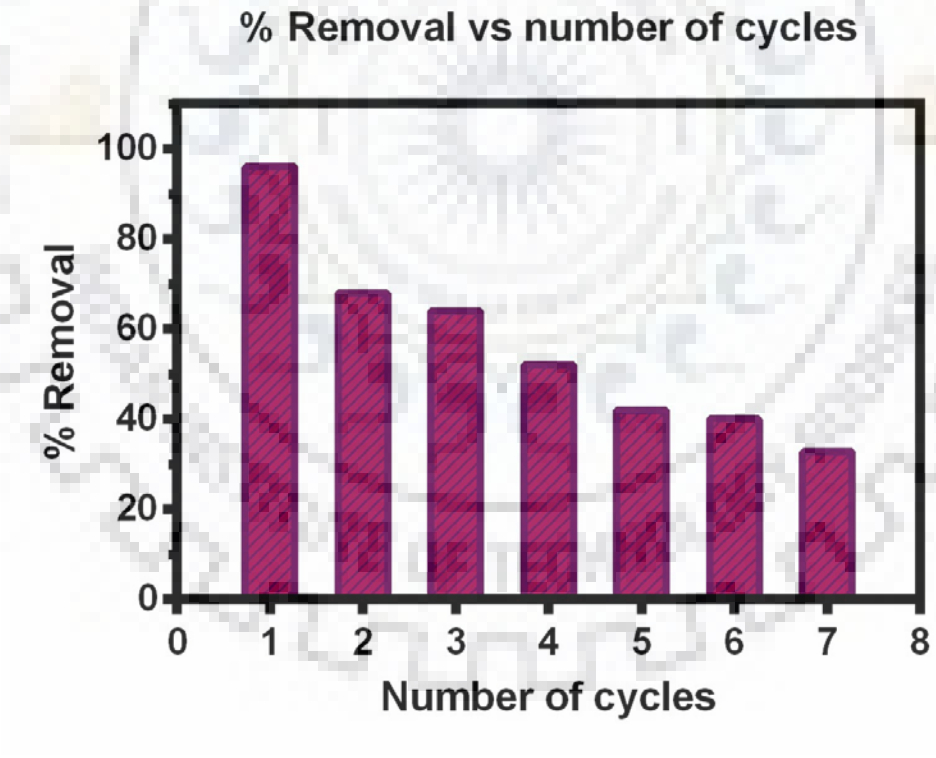

Figure 29 Reusability studies of PAN/MO nanofibers

CHAPTER 5 CONCLUSION

5.1 Conclusion

The MO loaded sodium alginate beads and PAN/MO nanofibers were. synthesized successfully. For beads, the concentration of Moringa oleifera was optimized to achieve better adsorption capacities. The beads and nanofibers were characterised using various analytical techniques. The adsorption experiments revealed that both beads and fibers have very similar adsorption capacities although fibers showed better adsorption capacity for higher concentrations of Congo Red. The kinetic studies revealed that both beads and fibers are in better agreement with pseudo-second order which suggests that the mechanism of adsorption is chemisorption. Isothermal studies shows that beads are in better agreement with Langmuir isotherm and fibers in Freundlich isotherm. Effect of Ph shows that the highest adsorption for both beads and fibers were under acidic conditions. The reusability studies showed that they still retained half their adsorption capacity after 7 days.

5.2 Future scope of work

The future scope of the present thesis is as follows.

- Further improvement of the construction of nanomaterials, the Na Alg/MO beads can be encapsulated with the iron oxide nanoparticles for the magnetic separation of the adsorbents after treatment.

- Apart from this, compartments for the loading of hybrid beads can be designed for the effective treatment.
- In the case of PAN/MO nanofibers, the nanofibrous sheets in the form of membrane can be developed through electrospinning according to the industrial specifications and it can be utilized in the reactor for the filtration as well as the adsorption process.
- Green synthesis of metal and metal oxide nanoparticles such as silver, iron, zinc, copper nanoparticles can be synthesized both from the seed as well as leaves. Further the nanoparticles can be loaded into the nanofibers for various applications.

REFERENCES

(1) Afroze, S., Sen, T.K., Ang, H.M., 2016. Adsorption performance of continuous fixed bed column for the removal of methylene blue (MB) dye using Eucalyptus sheathiana bark biomass. Res. Chem. Intermed. https://doi.org/10.1007/s11164-015-2153-8

(2) Ali, E.N., Muyibi, S. a, Salleh, H.M., Salleh, M.R.M., Islamic, I., 2010. Production Technique of Natural Coagulant From Moringa oleifera seeds. Fourteenth Int. Water Technol. Conf.

(3) Annadurai, G., Juang, R.S., Lee, D.J., 2002. Use of cellulose-based wastes for adsorption of dyes from aqueous solutions. J. Hazard. Mater. https://doi.org/10.1016/S0304-3894(02)00017-1

(4) Araújo, C.S.T., Melo, E.I., Alves, V.N., Coelho, N.M.M., 2010. Moringa oleifera Lam.
seeds as a natural solid adsorbent for removal of AgI in aqueous solutions. J. Braz. Chem. Soc. https://doi.org/10.1590/S0103-50532010000900019

(5) Bello, O.S., Adegoke, K.A., Akinyunni, O.O., 2017. Preparation and characterization of a novel adsorbent from Moringa oleifera leaf. Appl. Water Sci. 7, 1295–1305. https://doi.org/10.1007/s13201-015-0345-4

(6) Beltrán-Heredia, J., Sánchez-Martín, J., Delgado-Regalado, A., 2009. Removal of dyes by Moringa oleifera seed extract. Study through response surface methodology. J. Chem. Technol. Biotechnol. https://doi.org/10.1002/jctb.2225

(7) Bharathi, K.S., Ramesh, S.T., 2013. Removal of dyes using agricultural waste as lowcost adsorbents: a review. Appl. Water Sci. https://doi.org/10.1007/s13201-013-0117y

(8) Buczek, B., 2016. Preparation of Active Carbon by Additional Activation with Potassium Hydroxide and Characterization of Their Properties. Adv. Mater. Sci. Eng. https://doi.org/10.1155/2016/5819208

(9) Cardoso, N.F., Lima, E.C., Calvete, T., Pinto, I.S., Amavisca, C. V., Fernandes, T.H.M., Pinto, R.B., Alencar, W.S., 2011. Application of aqai stalks as biosorbents for the removal of the dyes reactive black 5 and reactive orange 16 from aqueous solution. J. Chem. Eng. Data. https://doi.org/10.1021/je100866c

(10) Cheah, W.K., Ishikawa, K., Othman, R., Yeoh, F.Y., 2017. Nanoporous biomaterials for uremic toxin adsorption in artificial kidney systems: A review. J. Biomed. Mater. Res. - Part B Appl. Biomater. https://doi.org/10.1002/jbm.b.33475

(11) Dahiru, M., Uba Zango, Z., Haruna, M.A., 2018. Cationic Dyes Removal Using LowCost Banana Peel Biosorbent. Am. J. Mater. Sci. https://doi.org/10.5923/j.materials.20180802.02

(12) de Castro, K.C., Cossolin, A.S., Oliveira dos Reis, H.C., de Morais, E.B., 2017. Biosorption of anionic textile dyes from aqueous solution by yeast slurry from brewery. Brazilian Arch. Biol. Technol. https://doi.org/10.1590/1678-4324-2017160101

(13) Eman N. Ali, Suleyman A. Muyibi, Hamzah M. Salleh, M.R.M.S. and M.Z.A., 2009. Moringa Oleifera Seeds As Natural Coagulant for Water TreatmentMoringa Oleifera Seeds As Natural Coagulant for Water Treatment. Water Technol. https://doi.org/10.1016/j.compstruct.2017.05.030

(14) Gao, S., Zhang, W., An, Z., Kong, S., Chen, D., 2019. Adsorption of anionic dye onto magnetic Fe_3O_4/CeO_2 nanocomposite: Equilibrium, kinetics, and thermodynamics. Adsorpt. Sci. Technol. 37, 185–204. https://doi.org/10.1177/0263617418819164

(15) Geçgel, Ü., Özcan, G., Gürpnar, G.Ç., 2013. Removal of methylene blue from aqueous solution by activated carbon prepared from pea shells (Pisum sativum). J. Chem.
https://doi.org/10.1155/2013/614083

(16) Ghaedi, M., Ghaedi, A.M., Abdi, F., Roosta, M., Vafaei, A., Asghari, A., 2013. Principal component analysis- adaptive neuro-fuzzy inference system modeling and

genetic algorithm optimization of adsorption of methylene blue by activated carbon derived from Pistacia khinjuk. Ecotoxicol. Environ. Saf. 96, 110–117. https://doi.org/10.1016/J.ECOENV.2013.05.015

(17) Ghasemzadeh, G., Momenpour, M., Omidi, F., Hosseini, M.R., Ahani, M., Barzegari, A., 2014. Applications of nanomaterials in water treatment and environmental remediation. Front. Environ. Sci. Eng. https://doi.org/10.1007/s11783-014-0654-0

(18) González-Horta, C., Ballinas-Casarrubias, L., Sánchez-Ramírez, B., Ishida, M.C., Barrera-Hernández, A., Gutiérrez-Torres, D., Zacarias, O.L., Saunders, R.J., Drobná, Z., Mendez, M.A., García-Vargas, G., Loomis, D., Stýblo, M., Del Razo, L.M., 2015. A concurrent exposure to arsenic and fluoride from drinking water in Chihuahua, Mexico. Int. J. Environ. Res. Public Health 12, 4587–601. https://doi.org/10.3390/ijerph120504587

(19) Gupta, V.K., Kumar, R., Nayak, A., Saleh, T.A., Barakat, M.A., 2013. Adsorptive removal of dyes from aqueous solution onto carbon nanotubes: A review. Adv. Colloid Interface Sci. https://doi.org/10.1016/j.cis.2013.03.003

(20) Kakunuri, M., Khandelwal, M., Sharma, C.S., Eichhorn, S.J., 2017. Fabrication of bioinspired hydrophobic self-assembled electrospun nanofiber based hierarchical structures. Mater. Lett. https://doi.org/10.1016/j.matlet.2017.03.094

(21) Keller, A.A., Garner, K., Miller, R.J., Lenihan, H.S., 2012. Toxicity of nano-zero valent iron to freshwater and marine organisms. PLoS One. https://doi.org/10.1371/journal.pone.0043983

(22) Kyzas, G.Z., Fu, J., Matis, K.A., 2013. The change from past to future for adsorbent materials in treatment of dyeing wastewaters. Materials (Basel). https://doi.org/10.3390/ma6115131

(23) Lee, L.Y., Chin, D.Z.B., Lee, X.J., Chemmangattuvalappil, N., Gan, S., 2015. Evaluation of Abelmoschus esculentus (lady's finger) seed as a novel biosorbent for the removal of Acid Blue 113 dye from aqueous solutions. Process Saf. Environ. Prot. https://doi.org/10.1016/j.psep.2014.08.004

(24) Liu, Y., Chen, X., Li, J., Burda, C., 2005. Photocatalytic degradation of azo dyes by nitrogen-doped TiO2 nanocatalysts. Chemosphere. https://doi.org/10.1016/j.chemosphere.2005.03.069

(25) Lu, Z., Hu, W., Xie, F., Hao, Y., 2017. Highly improved mechanical strength of aramid paper composite via a bridge of cellulose nanofiber. Cellulose. https://doi.org/10.1007/s10570-017-1315-9

(26) Mafra, M.R., Igarashi-Mafra, L., Zuim, D.R., Vasques, É.C., Ferreira, M.A., 2013. Adsorption of remazol brilliant blue on an orange peel adsorbent. Brazilian J. Chem. Eng. https://doi.org/10.1590/S0104-66322013000300022

(27) Malik, P.K., 2004. Dye removal from wastewater using activated carbon developed from sawdust: Adsorption equilibrium and kinetics. J. Hazard. Mater. https://doi.org/10.1016/j.jhazmat.2004.05.022

(28) Mallampati, R., Xuanjun, L., Adin, A., Valiyaveettil, S., 2015. Fruit peels as efficient renewable adsorbents for removal of dissolved heavy metals and dyes from water. ACS Sustain. Chem. Eng. https://doi.org/10.1021/acssuschemeng.5b00207

(29) Malwal, D., Gopinath, P., 2016. Fabrication and applications of ceramic nanofibers in water remediation: A review. Crit. Rev. Environ. Sci. Technol. https://doi.org/10.1080/10643389.2015.1109913

(30) Momina, Shahadat, M., Isamil, S., 2018. Regeneration performance of clay-based adsorbents for the removal of industrial dyes: A review. RSC Adv. https://doi.org/10.1039/c8ra04290j

(31) Patel, H., Vashi, R.T., 2012. Removal of Congo Red dye from its aqueous solution using natural coagulants. J. Saudi Chem. Soc. https://doi.org/10.1016/j.jscs.2010.12.003

(32) Puyol, D., Batstone, D.J., Hülsen, T., Astals, S., Peces, M., Krömer, J.O., 2017. Resource recovery from wastewater by biological technologies: Opportunities, challenges, and prospects. Front. Microbiol. https://doi.org/10.3389/fmicb.2016.02106

(33) Removal of heavy metals by natural adsorbent: review, 2014. . Int. J. Biosci. 130–139. https://doi.org/10.12692/ijb/4.7.130-139

(34) Safa, Y., Bhatti, H.N., 2011. Adsorptive removal of direct textile dyes by low cost agricultural waste: Application of factorial design analysis. Chem. Eng. J. https://doi.org/10.1016/j.cej.2010.11.103

(35) Saratale, R.G., Saratale, G.D., Chang, J.S., Govindwar, S.P., 2011. Bacterial decolorization and degradation of azo dyes: A review. J. Taiwan Inst. Chem. Eng. 42, 138–157. https://doi.org/10.1016/j.jtice.2010.06.006

(36) Saroj, S., Kumar, K., Pareek, N., Prasad, R., Singh, R.P., 2014. Biodegradation of azo dyes Acid Red 183, Direct Blue 15 and Direct Red 75 by the isolate Penicillium oxalicum SAR-3. Chemosphere. https://doi.org/10.1016/j.chemosphere.2013.12.049

(37) Soliman, N.K., Moustafa, A.F., Aboud, A.A., Halim, K.S.A., 2019. Effective utilization of Moringa seeds waste as anew green environmental adsorbent for removal ofindustrial toxic dyes. J. Mater. Res. Technol. https://doi.org/10.1016/j.jmrt.2018.12.010

(38) Suleyman A. Muyibi,, Megat, 2018. Conventional Treatment of Surface Water Using Moringa Oleifera Seeds Extract as a Primary Coagulant. IIUM Eng. J. https://doi.org/10.31436/iiumej.v5i1.375

(39) Taha, N.A., El-Maghraby, A., 2016. Magnetic peanut hulls for methylene blue dye removal: Isotherm and kinetic study. Glob. Nest J.

(40) Tan, K.B., Vakili, M., Horri, B.A., Poh, P.E., Abdullah, A.Z., Salamatinia, B., 2015a. Adsorption of dyes by nanomaterials: Recent developments and adsorption mechanisms. Sep. Purif. Technol. 150, 229–242. https://doi.org/10.1016/j.seppur.2015.07.009

(41) Tan, K.B., Vakili, M., Horri, B.A., Poh, P.E., Abdullah, A.Z., Salamatinia, B., 2015b. Adsorption of dyes by nanomaterials: Recent developments and adsorption mechanisms. Sep. Purif. Technol. https://doi.org/10.1016/j.seppur.2015.07.009

(42) Tie, J., Li, P., Xu, Z., Zhou, Y., Li, C., Zhang, X., 2015. Removal of Congo red from aqueous solution using Moringa oleifera seed cake as natural coagulant. Desalin. Water Treat. https://doi.org/10.1080/19443994.2014.905980

(43) Vieira, R.B., Vieira, P.A., Cardoso, S.L., Ribeiro, E.J., Cardoso, V.L., 2012. Sedimentation of mixed cultures using natural coagulants for the treatment of effluents generated in terrestrial fuel distribution terminals. J. Hazard. Mater. https://doi.org/10.1016/j.jhazmat.2012.06.043

(44) Vijayaraghavan, G., Shanthakumar, S., 2015. Efficacy of Moringa oleifera and Phaseolus vulgaris (common bean) as coagulants for the removal of Congo red dye from aqueous solution. J. Mater. Environ. Sci.

(45) Weber, C.T., Foletto, E.L., Meili, L., 2013. Removal of tannery dye from aqueous solution using papaya seed as an efficient natural biosorbent. Water. Air. Soil Pollut. https://doi.org/10.1007/s11270-012-1427-7